American Journal of Engineering and Applied Sciences

Original Research Paper

Kinetostatics of a 2T9R Robot Mechanism

Florian Ion Tiberiu Petrescu and Adriana Comanescu

ARoTMM-IFToMM, Bucharest Polytechnic University, Bucharest, (CE) Romania

Article history
Received: 18-01-2021
Revised: 22-08-2021
Accepted: 22-09-2021

Corresponding Author:
Florian Ion Tiberiu Petrescu
ARoTMM-IFToMM,
Bucharest Polytechnic University, Bucharest, (CE) Romania
Email: tiberiuflorianion@gmail.com

Abstract: The paper presents in detail a method of calculating the forces acting on a 2T9R type robot. To determine the reactions (forces in the kinematic couples), one must first determine the inertial forces in the mechanism to which one or more useful loads of the robot can be added. The torsor of the inertia forces is calculated with the help of the masses of the machine elements and the accelerations from the centers of mass of the mechanism elements, so the positions, velocities, and accelerations acting on it will be determined, i.e., its complete kinematics. The calculation method applied by a Math Cad program intelligently uses data entry through the If Log logic function so that the calculations can be automated. So, the effective automation of the calculation program is done exclusively through the If Log functions originally used in the paper.

Keywords: If Log, Robot, 2T9R Robot, Forces, Kinematics, Geometric-Analytical Method, Direct Kinematics, Inverse Kinematics

Introduction

Robots have always fascinated us, but today we use them massively, in almost all industrial areas, especially where they work hard, repetitive and tiring, in toxic, chemical, radioactive environments, underwater, in the cosmos, in dangerous environments, on mined lands, in hard-to-reach areas, etc. It can be said once again that, just as software and microchips have helped us to quickly write various useful programs and implement them directly, so robotics has made our daily work much easier. Thanks to robots, automation is almost perfect today, product quality is very high, the manufacturing price has dropped a lot, you can work in continuous fire, people have escaped hard work, tiring, repetitive, in toxic environments and now can treat other problems more important, such as design, scientific research, to work only 5 days a week with high income and, in the future, due to the massive implementation of increasingly modern robots with increased capabilities, man will reach the work week only 4 days.

An even greater increase is expected in the number of specialized robots implemented in large factories and factories around the world.

Due to the massive use of industrial robots, the diversification in this field has gained high levels. For this reason, we want to study in this study a new robot model, 2T9R, extremely complex in movements, useful in any type of work, and a versatile robot, which can weld, cut, process different parts, assemble them, or manipulate them from one working strip to another and in the same way, he can also paint the different machined components before their assembly. The robot has various advantages due to its complex mode arranged since the design and will be able to easily adapt to any type of automated manufacturing cell. For this reason and because it is an original one and has not been studied before, we want that in this study we review its study completely with the determination of all the forces that act it and that appear within it, the one that it also requires a complete kinematic calculation (Anderson, 1997; CEUP, 2018; García, 2020; Rana, 2020; Garfo *et al*., 2020; Kumar and Sreenivasulu, 2019; Mishra and Sarawagi, 2020; Welabo and Tesfamariamr, 2020; Antonescu and Petrescu, 1985; 1989; Antonescu *et al*., 1985a; 1985b; 1986; 1987; 1988; 1994; 1997; 2000a; 2000b; 2001; Aversa *et al*., 2017a; 2017b; 2017c; 2017d; 2016a; 2016b; 2016c; 2016d; Ayiei, 2020; Brewer, 1991; Chilukuri *et al*., 2019; Cao *et al*., 2013; Dong *et al*., 2013; Saheed *et al*., 2019; Riman, 2019; Matthews and Yi, 2019; Dwivedi *et al*., 2019a; 2019b; Eremia, 2020; Franklin, 1930; Hanrahan, 2014; He *et al*., 2013; Hertel, 2017; Komakula, 2019; Langston, 2015; 2016; Lee, 2013; Lin *et al*., 2013; Liu *et al*., 2013; Padula and Perdereau, 2013; Perumaal and Jawahar, 2013; Petrescu, 2011;

2012; 2019a-v; 2020a-g; Petrescu and Petrescu, 2019a-f; 1995a-b; 1997a-c; 2000a-b; 2002a-b; 2003; 2005a-e; 2011a-c; 2012a-b; 2013a-e; 2014a-h; 2016a-c; 2020; Petrescu *et al*., 2007; 2009; 2016; 2017a-ak; 2018a-w; 2020; Petrescu and Calautit, 2016a-b; Dekkata and Yi, 2019; Fahim *et al*., 2019; El Hassouni *et al*., 2019; Riman, 2018; Nacy and Nayif, 2018; Kortam *et al*., 2018; Welch and Mondal, 2019; Eissa *et al*., 2019; Younes *et al*., 2019; Svensson *et al*., 2004; Rahman, 2018; Richmond, 2013; Kisabo *et al*., 2019a; 2019b; Kisabo and Adebimpe, 2019; Kosambe, 2019a-d; Sharma and Kosambe, 2020; Oni and Jha, 2019; Chaudhary and Kumar, 2019; de Lima *et al*., 2019; Babu *et al*., 2019; 2020; de Mota Siqueira *et al*., 2020; Tumino, 2020; Mishra, 2020a; 2020b; Brischetto and Torre, 2020; Vladescu, 2020).

Materials and Methods

The present study will start with a description of the 2T9R robot proposed to be analyzed, in terms of the forces acting on it. The 2T9R mechanism (Fig. 1) has a constructive model based on a bimobile kinematic chain having three independent contours (Fig. 2a) obtained from the bicontour chain of the 2T6R mechanism.

The direct structural model (Fig. 2b) consists of two initial active modular groups GMAI (A, 1) and GMAI (G, 8) which constitute the linear motors that drive it, and two passive modular groups, one of the types of the GMP2 triad (2, 3,4,6) and the other of the GMP1 dyad type (5,7). The connection of the modular groups for the direct model is shown in Fig. 3.

The direct structural model (Fig. 2b) and the connection of the corresponding modular groups (Fig. 3) are used to determine the reaction torsor in each kinematic coupling using the kinetostatic principle.

To study the main plane mechanism of the 2T9R robot, its kinematic elements, kinematic torques, and positioning angles of the elements that also have rotation are initially established (Fig. 4).

For the kinetostatic analysis (determination of the forces in the mechanism) the centers of mass marked with the letter T (Fig. 5) are positioned as follows: O ≡ T5 ≡ T4; B ≡ T2 ≡ T3; E ≡ T6; F ≡ T7. Their placement does not influence the algorithm for calculating the components of the reaction torsion in the kinematic torques.

It is considered a single external force RT acting on the system neglecting other external forces (for example-gravitational forces). This simplification brings some peculiarities in the form of terms from the calculation algorithm without restricting its generality. The forces of weight are not recommended to be introduced in the sizing calculations because their influence is sometimes by addition and sometimes by decrease it being therefore opposite and having negative effects on the sizing of a mechanism.

On the other hand, in large (large) robots, if they still work fast (at high speeds), the inertial forces (internal forces, which arise even in the mechanism due to its masses) are considerable and much higher than those weights that automatically become negligible.

Determination of Reactions in the Kinematic Torques of the Triad (2,3,4,6)

The study of forces is always processed inversely to the kinematic one, i.e., not from the motors to the final effector element, but inversely, from the modular group furthest from the motors to them. For this reason, the force calculations start on the triad (2,3,4,6) from Fig. 6.

To determine the unknown forces, the reactions (from the kinematic couplings), the following calculation relations are written (from 2 ROx is made explicit, from 3 RAx, which is introduced in relation 1 and I am obtained and in relation 4 and II is obtained, where I and II represent two linear equations with two unknowns that make up a linear system that can be solved immediately by Kramer III):

$$\begin{cases} \sum M_E^{Tr} = 0 \\ M_4^i + R_O^x \cdot (y_E - y_O) - R_O^y \cdot (x_E - x_O) + R_A^x \cdot (y_E - y_A) - R_A^y \cdot (x_E - x_A) + \\ M_6^i + M_{23}^i + F_{T23}^{ix} \cdot (y_E - y_B) - F_{T23}^{iy} \cdot (x_E - x_B) + R_T \cdot (x_T - x_E) = 0 \end{cases} \tag{1}$$

$$\begin{cases} \sum M_C^{(4)} = 0 \\ M_4^i - R_O^x \cdot (y_O - y_C) - R_O^y \cdot (x_C - x_O) = 0 \end{cases} \tag{2}$$

$$\begin{cases} \sum M_B^{(2)} = 0 \\ M_2^i - R_A^x \cdot (y_A - y_B) - R_A^y \cdot (x_B - x_A) = 0 \end{cases} \tag{3}$$

$$\begin{cases} \sum M_D^{(4,3,2)} = 0 \\ M_4^i + M_{23}^i + R_O^x \cdot (y_D - y_O) - R_O^y \cdot (x_D - x_O) - R_A^x \cdot (y_A - y_D) - R_A^y \cdot (x_D - x_A) + \\ F_{T23}^{ix} \cdot (y_D - y_B) - F_{T23}^{iy} \cdot (x_D - x_B) = 0 \end{cases} \tag{4}$$

$$\begin{cases} \sum F_x^{(4,3,2,6)} = 0 \\ R_O^x + R_A^x + R_E^x + F_{T23}^{ix} + F_{T6}^{ix} = 0 \end{cases} \tag{5}$$

$$\begin{cases} \sum F_y^{(4,3,2,6)} = 0 \\ R_O^y + R_A^y + R_E^y + F_{T23}^{iy} + F_{T6}^{iy} + R_T = 0 \end{cases} \tag{6}$$

$$\begin{cases} R_O^y \cdot \left[(x_O - x_E) + \dfrac{(x_O - x_C) \cdot (y_E - y_O)}{(y_O - y_C)} \right] + R_A^y \cdot \left[(x_A - x_E) + \dfrac{(x_A - x_B) \cdot (y_E - y_A)}{(y_A - y_B)} \right] \\ = M_4^i \dfrac{(y_O - y_E)}{(y_O - y_C)} + M_2^i \dfrac{(y_A - y_E)}{(y_A - y_B)} - M_4^i - M_6^i - M_{23}^i + F_{T23}^{ix} \cdot (y_B - y_E) + \\ F_{T23}^{iy} \cdot (x_E - x_B) + R_T \cdot (x_E - x_T) \end{cases} \tag{I}$$

$$\begin{cases} R_O^y \cdot \left[\left(x_O - x_D \right) + \dfrac{\left(x_O - x_C \right) \cdot \left(y_D - y_O \right)}{\left(y_O - y_C \right)} \right] + R_A^y \cdot \left[\left(x_A - x_D \right) + \dfrac{\left(x_A - x_B \right) \cdot \left(y_D - y_A \right)}{\left(y_A - y_B \right)} \right] \\ = M_4^i \dfrac{\left(y_O - y_D \right)}{\left(y_O - y_C \right)} + M_2^i \dfrac{\left(y_A - y_D \right)}{\left(y_A - y_B \right)} - M_4^i - M_{23}^i + F_{T23}^{ix} \cdot \left(y_B - y_D \right) + F_{T23}^{iy} \cdot \left(x_D - x_B \right) \end{cases} \quad \text{(II)}$$

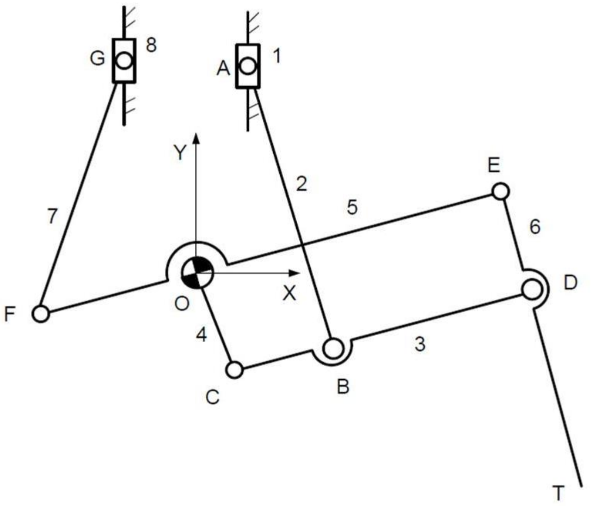

Fig. 1: The mechanism 2T9R

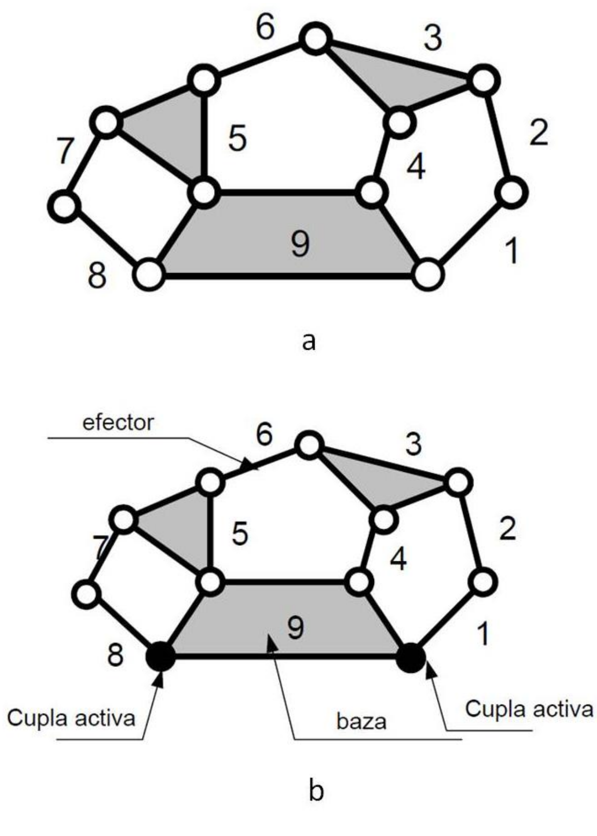

Fig. 2: Structural scheme of the mechanism

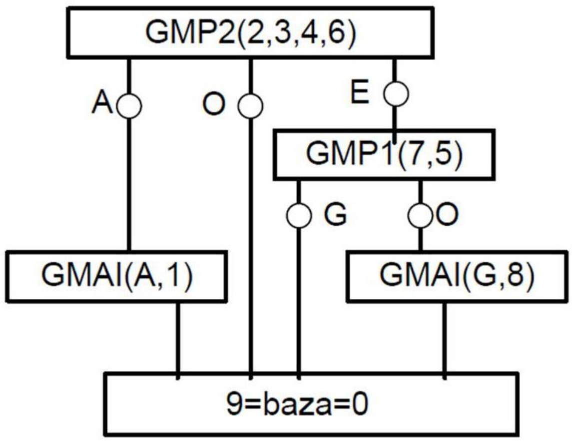

Fig. 3: Electronic or wiring diagram (block diagram) of the mechanism

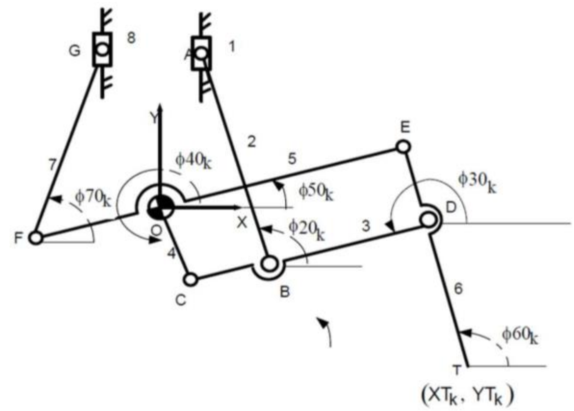

Fig. 4: Determining the kinematic elements, the kinematic torques, and the angles that position the elements that also have a rotation

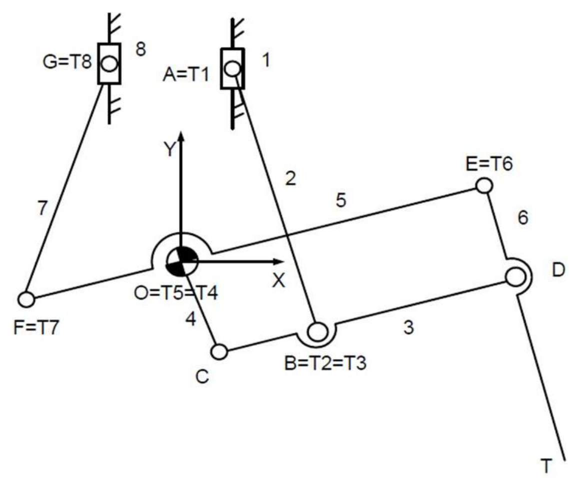

Fig. 5: Positioning the centers of mass T of all the elements of the mechanism

DOI: 10.3844/ajeassp.2022.59.80

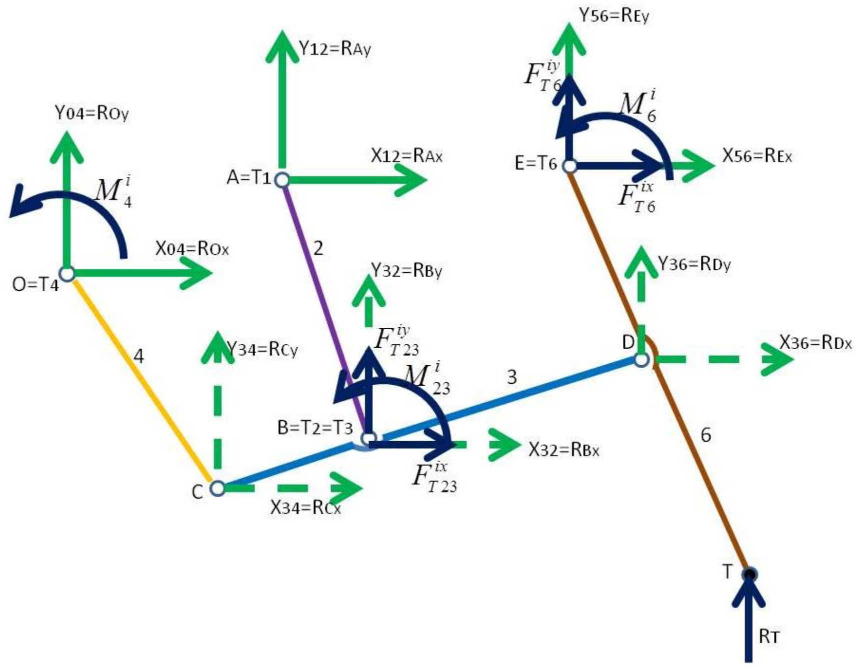

Fig. 6: The forces on the triad (2,3,4,6). The known forces are shown in blue; the reactions (unknown forces in the kinematic couplings) are drawn in green

From (5) results relation (V) which determines R_{Ex} and from (6) results in the expression (VI) which generates R_{Ey}:

$$\begin{cases} \begin{cases} a_{11}\cdot R_O^y + a_{12}\cdot R_A^y = a_1 \\ a_{21}\cdot R_O^y + a_{22}\cdot R_A^y = a_2 \end{cases} \\ a_{11} = (x_O - x_E) + \dfrac{(x_O - x_C)\cdot(y_E - y_O)}{(y_O - y_C)} \\ a_{12} = (x_A - x_E) + \dfrac{(x_A - x_B)\cdot(y_E - y_A)}{(y_A - y_B)} \\ a_1 = M_4^i \dfrac{(y_O - y_E)}{(y_O - y_C)} + M_2^i \dfrac{(y_A - y_E)}{(y_A - y_B)} - M_4^i - M_6^i - M_{23}^i + F_{T23}^{ix}\cdot(y_B - y_E) + \\ F_{T23}^{iy}\cdot(x_E - x_B) + R_T\cdot(x_E - x_T) \\ a_{21} = (x_O - x_D) + \dfrac{(x_O - x_C)\cdot(y_D - y_O)}{(y_O - y_C)} \\ a_{22} = (x_A - x_D) + \dfrac{(x_A - x_B)\cdot(y_D - y_A)}{(y_A - y_B)} \\ a_2 = M_4^i \dfrac{(y_O - y_D)}{(y_O - y_C)} + M_2^i \dfrac{(y_A - y_D)}{(y_A - y_B)} - M_4^i - M_{23}^i + F_{T23}^{ix}\cdot(y_B - y_D) + F_{T23}^{iy}\cdot(x_D - x_B) \\ \Delta = \begin{vmatrix} a_{11} & a_{12} \\ a_{21} & a_{22} \end{vmatrix} = a_{11}\cdot a_{22} - a_{12}\cdot a_{21} \, \Delta_O = \begin{vmatrix} a_1 & a_{12} \\ a_2 & a_{22} \end{vmatrix} = a_1\cdot a_{22} - a_{12}\cdot a_2 \\ \Delta_A = \begin{vmatrix} a_{11} & a_1 \\ a_{21} & a_2 \end{vmatrix} = a_{11}\cdot a_2 - a_1\cdot a_{21} R_O^y = \dfrac{\Delta_O}{\Delta}; R_A^y = \dfrac{\Delta_A}{\Delta} \end{cases} \tag{III}$$

With (IV) on determines R_{Ox} si R_{Ax}:

$$\begin{cases} R_O^x = \dfrac{M_4^i + R_O^y\cdot(x_O - x_C)}{(y_O - y_C)} \\ R_A^x = \dfrac{M_2^i + R_A^y\cdot(x_A - x_B)}{(y_A - y_B)} \end{cases} \tag{IV}$$

$$R_E^x = -\left(R_O^x + R_A^x + F_{T23}^{ix} + F_{T6}^{ix}\right) \tag{V}$$

$$R_E^y = -\left(R_O^y + R_A^y + F_{T23}^{iy} + F_{T6}^{iy} + R_T\right) \tag{VI}$$

Can now write the next equations (7-15):

$$\sum F_x^{(4)} = 0 \Rightarrow R_C^x \equiv X_{34} = -\left(R_O^x\right) \Rightarrow X_{43} = -X_{34} = R_O^x \tag{7}$$

$$\sum F_y^{(4)} = 0 \Rightarrow R_C^y \equiv Y_{34} = -\left(R_O^y\right) \Rightarrow Y_{43} = -Y_{34} = R_O^y \tag{8}$$

$$\sum F_x^{(2)} = 0 \Rightarrow R_B^x \equiv X_{32} = -\left(R_A^x + F_{T2}^{ix}\right) \Rightarrow X_{23} = -X_{32} \tag{9}$$

$$\sum F_y^{(2)} = 0 \Rightarrow R_B^y \equiv Y_{32} = -\left(R_A^y + F_{T2}^{iy}\right) \Rightarrow Y_{23} = -Y_{32} \tag{10}$$

$$\sum F_x^{(6)} = 0 \Rightarrow R_D^x \equiv X_{36} = -\left(R_E^x + F_{T6}^{ix}\right) \Rightarrow X_{63} = -X_{36} \tag{11}$$

$$\sum F_y^{(6)} = 0 \Rightarrow R_D^y \equiv Y_{36} = -\left(R_E^y + F_{T6}^{iy} + R_T\right) \Rightarrow Y_{63} = -Y \tag{12}$$

$$X_{40} = -X_{04} = -R_O^x; Y_{40} = -Y_{04} = -R_O^y \tag{13}$$

$$X_{21} = -X_{12} = -R_A^x; Y_{21} = -Y_{12} = -R_A^y \tag{14}$$

$$X_{65} = -X_{56} = -R_E^x; Y_{65} = -Y_{56} = -R_E^y \tag{15}$$

To perform the triad calculations (2,3,4,6) it is necessary to present briefly the expressions by which the known inertial forces, inside the mechanism, due to the masses of the component elements (16-20) are determined by calculations:

$$M_4^i = -J_{T_4} \cdot \varepsilon_4 = -J_O^{(4)} \cdot \varepsilon_4 \tag{16}$$

$$\begin{cases} F_{T_2}^{ix} = -m_2 \cdot \ddot{x}_B \\ F_{T_2}^{iy} = -m_2 \cdot \ddot{y}_B \\ M_2^i = -J_B^{(2)} \cdot \varepsilon_2 \end{cases} \tag{17}$$

$$\begin{cases} F_{T_3}^{ix} = -m_3 \cdot \ddot{x}_B \\ F_{T_3}^{iy} = -m_3 \cdot \ddot{y}_B \\ M_3^i = -J_B^{(3)} \cdot \varepsilon_3 \end{cases} \tag{18}$$

$$\begin{cases} F_{T_{23}}^{ix} = F_{T_2}^{ix} + F_{T_3}^{ix} = -(m_2 + m_3) \cdot \ddot{x}_B \\ F_{T_{23}}^{iy} = F_{T_2}^{iy} + F_{T_3}^{iy} = -(m_2 + m_3) \cdot \ddot{y}_B \\ M_{23}^i = M_2^i + M_3^i = -J_B^{(2)} \cdot \varepsilon_2 - J_B^{(3)} \cdot \varepsilon_3 \end{cases} \tag{19}$$

$$\begin{cases} F_{T_6}^{ix} = -m_6 \cdot \ddot{x}_E \\ F_{T_6}^{iy} = -m_6 \cdot \ddot{y}_E \\ M_6^i = -J_E^{(6)} \cdot \varepsilon_6 \end{cases} \tag{20}$$

Determination of Reactions in the Kinematic Couplings of the Dyad (5,7)

Dyad 5.7 has the following charges (Fig. 7), where the already known forces are shown in blue and the unknown ones in green, i.e., the reactions in the kinematic torques of the dyad, which will be determined.

Can write the relations 21-22:

$$\begin{cases} \sum M_O^{(7,5)} = 0 \\ M_7^i + M_5^i - R_G^x \cdot (y_G - y_O) - R_G^y \cdot (x_O - x_G) + F_{T7}^{ix} \cdot (y_O - y_F) - F_{T7}^{iy} \cdot (x_O - x_F) \\ -X_{65} \cdot (y_E - y_O) + Y_{65} \cdot (x_E - x_O) = 0 \end{cases} \tag{21}$$

$$\begin{cases} \sum M_F^{(7)} = 0 \\ M_7^i - R_G^x \cdot (y_G - y_F) + R_G^y \cdot (x_G - x_F) = 0 \end{cases} \tag{22}$$

From relation (22) one explicitly reaction R_{Gy} (24) which is introduced in relation (21) obtaining directly the value R_{Gx} (23) and then R_{Gy} (24):

$$R_G^x = \frac{F_{T7}^{ix}(y_F - y_O) + F_{T7}^{iy}(x_O - x_F) + R_E^x(y_O - y_E) + R_E^y(x_E - x_O) - M_7^i - M_5^i + M_7^i \frac{(x_G - x_O)}{(x_G - x_F)}}{\frac{(y_O - y_G) \cdot (x_G - x_F) + (y_G - y_F) \cdot (x_G - x_O)}{(x_G - x_F)}} \tag{23}$$

$$R_G^y = \frac{R_G^x(y_G - y_F) - M_7^i}{(x_G - x_F)} \Rightarrow Y_{78} = -Y_{87} = -R_G^y \tag{24}$$

Now, one write the relations (25-30):

$$\sum F_x^{(7)} = 0 \Rightarrow R_F^x \equiv X_{57} = -\left(R_G^x + F_{T7}^{ix}\right) \Rightarrow X_{75} = -X_{57} \tag{25}$$

$$\sum F_y^{(7)} = 0 \Rightarrow R_F^y \equiv Y_{57} = -\left(R_G^y + F_{T7}^{iy}\right) \Rightarrow Y_{75} = -Y_{57} \tag{26}$$

$$\sum F_x^{(5)} = 0 \Rightarrow X_{05} = -\left(X_{65} + X_{75}\right) = R_E^x + R_F^x \tag{27}$$

$$\sum F_y^{(5)} = 0 \Rightarrow Y_{05} = -\left(Y_{65} + Y_{75}\right) = R_E^y + R_F^y \tag{28}$$

$$X_{50} \equiv -R'^x_O = -X_{05} = -(R_E^x + R_F^x) \tag{29}$$

$$Y_{50} \equiv -R'^y_O = -Y_{05} = -(R_E^y + R_F^y) \tag{30}$$

The torsor of the inertial forces on dyad 5,7 is determined by the relations (31-32):

$$M_5^i = -J_O^{(5)} \cdot \varepsilon_5 \tag{31}$$

$$\begin{cases} F_{T_7}^{ix} = -m_7 \cdot \ddot{x}_F \\ F_{T_7}^{iy} = -m_7 \cdot \ddot{y}_F \\ M_7^i = -J_F^{(7)} \cdot \varepsilon_7 \end{cases} \tag{32}$$

Determination of the Reactions in the Kinematic Torques of the Motor Element 8 and Calculation of the Driving Force Fm8

Figure 8 shows all the forces acting on the linear motor element 8, in the rotation torque G (between elements 8 and 7) and the translation torque T8 (between elements 8 and 0) materialized by the guideline between the motor piston 8 and its axis of vertical symmetry coinciding with the guide 0, considering as the point of actuation of the forces 08 the center of mass T8. The forces in the torque are the x-axis and y-axis projections of the already known R78 reaction (thus shown in dark blue). Also known as the torsion of the inertial forces on element 8, represented here only by an inertial force along the guide axis y (its action is concentrated in the center of mass T8), there is no movement on the x-axis acceleration and automatic and force inertial on this x-axis is canceled and the inertial moment is also canceled permanently because there is no rotational motion, the angular and automatic acceleration and the inertial moment being canceled.

The driving force that moves the linear motor element 8 also acts in the center of mass. Practically except for the reaction in coupling G all other forces act on the center of mass T8. Relationships can be written (33-36):

$$F_{T_8}^{iy} = -m_8 \cdot \ddot{y}_G \tag{33}$$

$$\sum F_x^{(8)} = 0 \Rightarrow X_{78} + N_{08} = 0 \Rightarrow N_{08} = -X_{78} \Rightarrow N_{08} = R_G^x \tag{34}$$

$$\sum F_y^{(8)} = 0 \Rightarrow F_{m8} + Y_{78} + F_{T_8}^{iy} = 0 \Rightarrow F_{m8} = -Y_{78} - F_{T_8}^{iy} \Rightarrow F_{m8} = R_G^y - F_{T_8}^{iy} \tag{35}$$

$$\sum M_{T_8}^{(8)} = 0 \Rightarrow M_{08} - X_{78} \cdot \left(y_G - y_{T_8}\right) = 0 \Rightarrow M_{08} = R_G^x \cdot \left(y_{T_8} - y_G\right) \tag{36}$$

It is specified here that if the points G and T8 coincide the moment M08 is canceled together with the phase shift $\left(\left(y_{T_8} - y_G\right) = 0\right)$.

The procedure is then repeated for engine 1 (Fig. 9, relations 37-40).

Determination of the Reactions in the Kinematic Torques of the Motor Element 1 and Calculation of the Driving Force Fm1

$$F_{T_1}^{iy} = -m_1 \cdot \ddot{y}_A \tag{37}$$

$$\sum F_x^{(1)} = 0 \Rightarrow X_{21} + N_{01} = 0 \Rightarrow N_{01} = -X_{21} \Rightarrow N_{01} = R_A^x \tag{38}$$

$$\sum F_y^{(1)} = 0 \Rightarrow F_{m1} + Y_{21} + F_{T_1}^{iy} = 0 \Rightarrow F_{m1} = -Y_{21} - F_{T_1}^{iy} \Rightarrow F_{m1} = R_A^y - F_{T_1}^{iy} \tag{39}$$

$$\sum M_{T_1}^{(1)} = 0 \Rightarrow M_{01} - X_{21} \cdot \left(y_A - y_{T_1}\right) = 0 \Rightarrow M_{01} = R_A^x \cdot \left(y_{T_1} - y_A\right) \tag{40}$$

It is specified that if points A and T1 coincide the moment M01 is canceled together with the phase shift $\left(\left(y_{T_1} - y_A\right) = 0\right)$.

Remarks: Any torque introduces a reaction that decomposes along the coordinate axes (in the plane) into two components along the *x* and *y* axes, while each translation torque introduces a reaction perpendicular to the torque guide axis and a moment.

Any reaction in any pair is easily determined by having the modulus (size) given by the radical in the sum of the squares of the two scalar components of the reaction and its position (the direction of the vector defining it) is given by an alpha angle measured from the horizontal which passes through the origin of the reaction (the respective coupling) and which has the trigonometric functions described by the two-component scalar and the vector of the respective reaction.

Determination of Robot Speeds and Accelerations

The kinematic calculation of the robot's speeds and accelerations is done only by direct kinematics as it is operated in reality, while the positions can be determined in two distinct situations, by direct kinematics when we are interested in the normal operation of the robot, finding the workspace. and the trajectories described by the effector element (or other component kinematic couplings), or by using inverse kinematics when the positions that the final element (effector) must occupy successively are already imposed and the successive positions of the driving elements must be determined, for this robot the linear motors 1 and 8.

Determination of Robot Speeds and Accelerations to the Dyad 5,7

As stated, only direct kinematics is used to determine speeds and accelerations, so the calculations from dyad 5.7 are started (Fig. 10).

Write the calculation relationships in the system (41):

The scalar coordinates, velocities, and accelerations of points G and O are known, with the help of which, using the equations of the two circles formed, the scalar coordinates of point F are determined. Then easily determine the angles FI5 and FI7 with their derivatives, ω_5,ε_5, ω_7,ε_7:

$$\begin{cases} (x_G - x_F)^2 + (y_G - y_F)^2 = i^2 \Rightarrow 2(x_G - x_F)\cdot(\dot{x}_G - \dot{x}_F) + 2(y_G - y_F)\cdot(\dot{y}_G - \dot{y}_F) = 0 \\ (x_F - x_O)^2 + (y_F - y_O)^2 = f^2; x_O = y_O = 0 \Rightarrow 2x_F \cdot \dot{x}_F + 2y_F \cdot \dot{y}_F \Rightarrow \dot{y}_F = -\dfrac{x_F \dot{x}_F}{y_F} \\ \dot{x}_F = \dfrac{(y_G - y_F)\cdot y_F \cdot \dot{y}_G}{(x_G - x_F)\cdot y_F - (y_G - y_F)\cdot x_F}; \omega_7 = \dfrac{\dot{y}_G - \dot{y}_F}{x_G - x_F}; \varepsilon_7 = \dfrac{\ddot{y}_G - \ddot{y}_F - \omega_7(\dot{x}_G - \dot{x}_F)}{x_G - x_F} \\ \dot{y}_F = \dfrac{-(y_G - y_F)\cdot x_F \cdot \dot{y}_G}{(x_G - x_F)\cdot y_F - (y_G - y_F)\cdot x_F} \Rightarrow \omega_5 = \dfrac{\dot{y}_F}{x_F} \Rightarrow \varepsilon_5 = \dfrac{\ddot{y}_F - \omega_5 \cdot \dot{x}_F}{x_F} \\ \ddot{x}_F = \dfrac{(\dot{y}_G - \dot{y}_F)\cdot y_F \cdot \dot{y}_G + (y_G - y_F)\cdot \dot{y}_F \cdot \dot{y}_G + (y_G - y_F)\cdot y_F \cdot \ddot{y}_G}{(x_G - x_F)\cdot y_F - (y_G - y_F)\cdot x_F} - \\ \dfrac{\dot{x}_F\left[(\dot{x}_G - \dot{x}_F)\cdot y_F - (\dot{y}_G - \dot{y}_F)\cdot x_F + (x_G - x_F)\cdot \dot{y}_F - (y_G - y_F)\cdot \dot{x}_F\right]}{(x_G - x_F)\cdot y_F - (y_G - y_F)\cdot x_F} \\ \ddot{y}_F = \dfrac{-\dot{x}_F^2 - \dot{y}_F^2 - x_F \cdot \ddot{x}_F}{y_F} \\ x_E = e\cdot\cos\phi_5 \Rightarrow \dot{x}_E = -e\cdot\sin\phi_5\cdot\omega_5 \Rightarrow \ddot{x}_E = -e\cdot\cos\phi_5\cdot\omega_5^2 - e\cdot\sin\phi_5\cdot\varepsilon_5 \\ y_E = e\cdot\sin\phi_5 \Rightarrow \dot{y}_E = e\cdot\cos\phi_5\cdot\omega_5 \Rightarrow \ddot{y}_E = -e\cdot\sin\phi_5\cdot\omega_5^2 + e\cdot\cos\phi_5\cdot\varepsilon_5 \end{cases} \tag{41}$$

Determination of Speeds and Accelerations in the Triad 2,3,4,6

In figure 11 you can see the positions with the sizes characteristic of triads 2,3,4,6 starting from which the relations of positions, speeds, and accelerations are written.

Position relations being considered already solved and all known position values (solved separately by direct or inverse kinematics as required), derived directly twice and thus obtaining triad speeds and accelerations (2,3,4,6), Eq. (42-52):

$$\begin{cases} \begin{cases} x_C = d\cdot\cos\phi_4 \\ y_C = d\cdot\sin\phi_4 \end{cases} \begin{cases} \dot{x}_C = -d\cdot\sin\phi_4\cdot\omega_4 \\ \dot{y}_C = d\cdot\cos\phi_4\cdot\omega_4 \end{cases} \begin{cases} x_B = x_A - a\cdot\cos\phi_2 \\ y_B = y_A - a\cdot\sin\phi_2 \end{cases} \begin{cases} \dot{x}_B = \dot{x}_A + a\cdot\sin\phi_2\cdot\omega_2 \\ \dot{y}_B = \dot{y}_A - a\cdot\cos\phi_2\cdot\omega_2 \end{cases} \\ \begin{cases} x_C = x_B + b\cos\phi_3 \\ y_C = y_B + b\sin\phi_3 \end{cases} \begin{cases} \dot{x}_C = \dot{x}_B - b\sin\phi_3\omega_3 \\ \dot{y}_C = \dot{y}_B + b\cos\phi_3\omega_3 \end{cases} \begin{cases} -d\sin\phi_4\omega_4 = \dot{x}_A + a\sin\phi_2\omega_2 - b\sin\phi_3\omega_3 \\ d\cos\phi_4\omega_4 = \dot{y}_A - a\cos\phi_2\omega_2 + b\cos\phi_3\omega_3 \end{cases} \\ \begin{cases} x_D = x_B - c\cos\phi_3 \\ y_D = y_B - c\sin\phi_3 \end{cases} \begin{cases} \dot{x}_D = \dot{x}_B + c\sin\phi_3\omega_3 \\ \dot{y}_D = \dot{y}_B - c\cos\phi_3\omega_3 \end{cases} \begin{cases} x_E = x_D + g\cos\phi_6 \\ y_E = y_D + g\sin\phi_6 \end{cases} \begin{cases} \dot{x}_E = \dot{x}_D - g\sin\phi_6\omega_6 \\ \dot{y}_E = \dot{y}_D + g\cos\phi_6\omega_6 \end{cases} \\ \begin{cases} \dot{x}_A - \dot{x}_E + a\cdot\sin\phi_2\cdot\omega_2 + c\cdot\sin\phi_3\cdot\omega_3 = g\cdot\sin\phi_6\cdot\omega_6 \\ \dot{y}_A - \dot{y}_E - a\cdot\cos\phi_2\cdot\omega_2 - c\cdot\cos\phi_3\cdot\omega_3 = -g\cdot\cos\phi_6\cdot\omega_6 \end{cases} \end{cases} \tag{42}$$

$$\begin{cases} \begin{cases} -d\cdot\sin\phi_4\cdot\omega_4 = \dot{x}_A + a\cdot\sin\phi_2\cdot\omega_2 - b\cdot\sin\phi_3\cdot\omega_3 \,|\cdot\cos\phi_4 \\ d\cdot\cos\phi_4\cdot\omega_4 = \dot{y}_A - a\cdot\cos\phi_2\cdot\omega_2 + b\cdot\cos\phi_3\cdot\omega_3 \,|\cdot\sin\phi_4 \end{cases} \Rightarrow I \\ \begin{cases} \dot{x}_A - \dot{x}_E + a\cdot\sin\phi_2\cdot\omega_2 + c\cdot\sin\phi_3\cdot\omega_3 = g\cdot\sin\phi_6\cdot\omega_6 \,|\cdot\cos\phi_6 \\ \dot{y}_A - \dot{y}_E - a\cdot\cos\phi_2\cdot\omega_2 - c\cdot\cos\phi_3\cdot\omega_3 = -g\cdot\cos\phi_6\cdot\omega_6 \,|\cdot\sin\phi_6 \end{cases} \Rightarrow II \\ \begin{cases} (I): \dot{x}_A\cdot\cos\phi_4 + \dot{y}_A\cdot\sin\phi_4 + a\cdot\omega_2\cdot\sin(\phi_2-\phi_4) + b\cdot\omega_3\cdot\sin(\phi_4-\phi_3) = 0 \\ (II): (\dot{x}_A-\dot{x}_E)\cos\phi_6 + (\dot{y}_A-\dot{y}_E)\sin\phi_6 + a\omega_2\sin(\phi_2-\phi_6) + c\omega_3\sin(\phi_3-\phi_6) = 0 \end{cases} \end{cases} \tag{43}$$

$$\begin{cases} \begin{cases} \dot{x}_A\cdot\cos\phi_4 + \dot{y}_A\cdot\sin\phi_4 + a\cdot\omega_2\cdot\sin(\phi_2-\phi_4) + b\cdot\omega_3\cdot\sin(\phi_4-\phi_3) = 0 \\ (\dot{x}_A-\dot{x}_E)\cos\phi_6 + (\dot{y}_A-\dot{y}_E)\sin\phi_6 + a\omega_2\sin(\phi_2-\phi_6) + c\omega_3\sin(\phi_3-\phi_6) = 0 \end{cases} \\ (I)\cdot[c\cdot\sin(\phi_3-\phi_6)](II)\cdot[-b\cdot\sin(\phi_4-\phi_3)] \Rightarrow \omega_2 \\ (I)\cdot[\sin(\phi_2-\phi_6)](II)\cdot[-\sin(\phi_2-\phi_4)] \Rightarrow \omega_3 \\ \omega_2 = \dfrac{b[(\dot{x}_A-\dot{x}_E)\cos\phi_6 + (\dot{y}_A-\dot{y}_E)\sin\phi_6]\sin(\phi_3-\phi_4) + c(\dot{x}_A\cos\phi_4 + \dot{y}_A\sin\phi_4)\sin(\phi_3-\phi_6)}{a\cdot[c\cdot\sin(\phi_2-\phi_4)\cdot\sin(\phi_6-\phi_3) + b\cdot\sin(\phi_2-\phi_6)\cdot\sin(\phi_4-\phi_3)]} \\ \omega_3 = \dfrac{[(\dot{x}_A-\dot{x}_E)\cos\phi_6 + (\dot{y}_A-\dot{y}_E)\sin\phi_6]\sin(\phi_2-\phi_4) + (\dot{x}_A\cos\phi_4 + \dot{y}_A\sin\phi_4)\sin(\phi_6-\phi_2)}{[c\cdot\sin(\phi_2-\phi_4)\cdot\sin(\phi_6-\phi_3) + b\cdot\sin(\phi_2-\phi_6)\cdot\sin(\phi_4-\phi_3)]} \\ \omega_4 = \dfrac{\dot{y}_A - \dot{x}_A - a\cdot\omega_2\cdot\cos(\phi_4-\phi_2) + b\cdot\omega_3\cdot\cos(\phi_4-\phi_3)}{d} \\ \omega_6 = \dfrac{\dot{x}_A - \dot{x}_E + \dot{y}_E - \dot{y}_A + a\cdot\omega_2\cdot\cos(\phi_6-\phi_2) + c\cdot\omega_3\cdot\cos(\phi_6-\phi_3)}{g} \\ \begin{cases} \dot{x}_C = -d\sin\phi_4\omega_4 \\ \dot{y}_C = d\cos\phi_4\omega_4 \end{cases} \begin{cases} \dot{x}_B = \dot{x}_A + a\sin\phi_2\omega_2 \\ \dot{y}_B = \dot{y}_A - a\cos\phi_2\omega_2 \end{cases} \begin{cases} \dot{x}_D = \dot{x}_B + c\sin\phi_3\omega_3 \\ \dot{y}_D = \dot{y}_B - c\cos\phi_3\omega_3 \end{cases} \begin{cases} \dot{x}_T = \dot{x}_D + h\sin\phi_6\omega_6 \\ \dot{y}_T = \dot{y}_D - h\cos\phi_6\omega_6 \end{cases} \end{cases} \tag{44}$$

$$\begin{cases} \varepsilon_2\cdot[ac\sin(\phi_2-\phi_4)\sin(\phi_6-\phi_3) + ab\sin(\phi_2-\phi_6)\sin(\phi_4-\phi_3)] = \\ = \omega_2\cdot[ac\cos(\phi_2-\phi_4)\sin(\phi_3-\phi_6)(\omega_2-\omega_4) + ac\sin(\phi_4-\phi_2)\cos(\phi_6-\phi_3)(\omega_6-\omega_3) + \\ ab\cos(\phi_2-\phi_6)\sin(\phi_3-\phi_4)(\omega_2-\omega_6) + ab\sin(\phi_6-\phi_2)\cos(\phi_4-\phi_3)(\omega_4-\omega_3)] + \\ [(\ddot{x}_A-\ddot{x}_E)\cos\phi_6 + (\dot{x}_E-\dot{x}_A)\sin\phi_6\omega_6 + (\ddot{y}_A-\ddot{y}_E)\sin\phi_6 + (\dot{y}_A-\dot{y}_E)\cos\phi_6\omega_6]b\sin(\phi_3-\phi_4) + \\ [(\dot{x}_A-\dot{x}_E)\cos\phi_6 + (\dot{y}_A-\dot{y}_E)\sin\phi_6]b\cos(\phi_3-\phi_4)(\omega_3-\omega_4) + (\ddot{x}_A\cos\phi_4 + \ddot{y}_A\sin\phi_4 - \\ \dot{x}_A\sin\phi_4\omega_4 + \dot{y}_A\cos\phi_4\omega_4)c\sin(\phi_3-\phi_6) + (\dot{x}_A\cos\phi_4 + \dot{y}_A\sin\phi_4)c\cos(\phi_3-\phi_6)(\omega_3-\omega_6) \end{cases} \tag{45}$$

$$\begin{cases} \varepsilon_3\cdot[b\sin(\phi_4-\phi_3)\sin(\phi_2-\phi_6) + c\sin(\phi_3-\phi_6)\sin(\phi_4-\phi_2)] = \\ = \omega_3\cdot[b\cos(\phi_4-\phi_3)\sin(\phi_6-\phi_2)(\omega_4-\omega_3) + b\sin(\phi_3-\phi_4)\cos(\phi_2-\phi_6)(\omega_2-\omega_6) + \\ c\cos(\phi_3-\phi_6)\sin(\phi_2-\phi_4)(\omega_3-\omega_6) + c\sin(\phi_6-\phi_3)\cos(\phi_4-\phi_2)(\omega_4-\omega_2)] + \\ (\ddot{x}_A\cos\phi_4 + \ddot{y}_A\sin\phi_4 - \dot{x}_A\sin\phi_4\omega_4 + \dot{y}_A\cos\phi_4\omega_4)\sin(\phi_6-\phi_2) + \\ (\dot{x}_A\cos\phi_4 + \dot{y}_A\sin\phi_4)\cos(\phi_6-\phi_2)(\omega_6-\omega_2) + \sin(\phi_2-\phi_4)\cdot[(\ddot{x}_A-\ddot{x}_E)\cos\phi_6 + \\ (\ddot{y}_A-\ddot{y}_E)\sin\phi_6 + (\dot{x}_E-\dot{x}_A)\sin\phi_6\omega_6 + (\dot{y}_A-\dot{y}_E)\cos\phi_6\omega_6] + \\ [(\dot{x}_A-\dot{x}_E)\cos\phi_6 + (\dot{y}_A-\dot{y}_E)\sin\phi_6]\cdot\cos(\phi_2-\phi_4)(\omega_2-\omega_4) \end{cases} \tag{46}$$

$$\begin{cases} \varepsilon_4\cdot d = \\ = (\ddot{y}_A + a\sin\phi_2\omega_2^2 - a\cos\phi_2\varepsilon_2 - b\sin\phi_3\omega_3^2 + b\cos\phi_3\varepsilon_3)\cos\phi_4 - \\ (\dot{y}_A - a\cos\phi_2\omega_2 + b\cos\phi_3\omega_3)\sin\phi_4\omega_4 - \sin\phi_4(\ddot{x}_A + a\cos\phi_2\omega_2^2 + a\sin\phi_2\varepsilon_2 - \\ b\cos\phi_3\omega_3^2 - b\sin\phi_3\varepsilon_3) - (\dot{x}_A + a\sin\phi_2\omega_2 - b\sin\phi_3\omega_3)\cos\phi_4\omega_4 \end{cases} \tag{47}$$

$$\begin{cases} \varepsilon_6\cdot g = \\ = (\ddot{x}_A - \ddot{x}_E + a\cos\phi_2\omega_2^2 + a\sin\phi_2\varepsilon_2 + c\cos\phi_3\omega_3^2 + c\sin\phi_3\varepsilon_3)\sin\phi_6 + \\ (\dot{x}_A - \dot{x}_E + a\sin\phi_2\omega_2 + c\sin\phi_3\omega_3)\cos\phi_6\omega_6 + \cos\phi_6(\ddot{y}_E - \ddot{y}_A - a\sin\phi_2\omega_2^2 + \\ a\cos\phi_2\varepsilon_2 - c\sin\phi_3\omega_3^2 + c\cos\phi_3\varepsilon_3) - (\dot{y}_E - \dot{y}_A + a\cos\phi_2\omega_2 + c\cos\phi_3\omega_3)\sin\phi_6\omega_6 \end{cases} \tag{48}$$

$$\begin{cases} \ddot{x}_C = -d\cdot\cos\phi_4\cdot\omega_4^2 - d\cdot\sin\phi_4\cdot\varepsilon_4 \\ \ddot{y}_C = -d\cdot\sin\phi_4\cdot\omega_4^2 + d\cdot\cos\phi_4\cdot\varepsilon_4 \end{cases} \tag{49}$$

$$\begin{cases} \ddot{x}_B = \ddot{x}_A + a\cdot\cos\phi_2\cdot\omega_2^2 + a\cdot\sin\phi_2\cdot\varepsilon_2 \\ \ddot{y}_B = \ddot{y}_A + a\cdot\sin\phi_2\cdot\omega_2^2 - a\cdot\cos\phi_2\cdot\varepsilon_2 \end{cases} \tag{50}$$

$$\begin{cases} \ddot{x}_D = \ddot{x}_E + g\cdot\cos\phi_6\cdot\omega_6^2 + g\cdot\sin\phi_6\cdot\varepsilon_6 \\ \ddot{y}_D = \ddot{y}_E + g\cdot\sin\phi_6\cdot\omega_6^2 - g\cdot\cos\phi_6\cdot\varepsilon_6 \end{cases} \tag{51}$$

$$\begin{cases} \ddot{x}_T = \ddot{x}_D + h\cdot\cos\phi_6\cdot\omega_6^2 + h\cdot\sin\phi_6\cdot\varepsilon_6 \\ \ddot{y}_T = \ddot{y}_D + h\cdot\sin\phi_6\cdot\omega_6^2 - h\cdot\cos\phi_6\cdot\varepsilon_6 \end{cases} \tag{52}$$

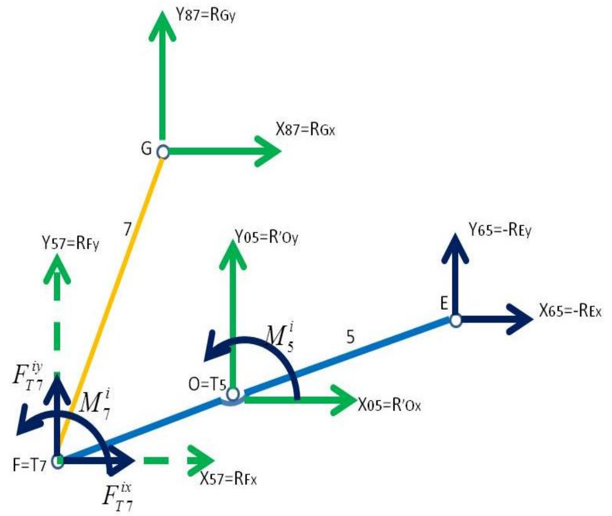

Fig. 7: Forces of the dyad 5-7

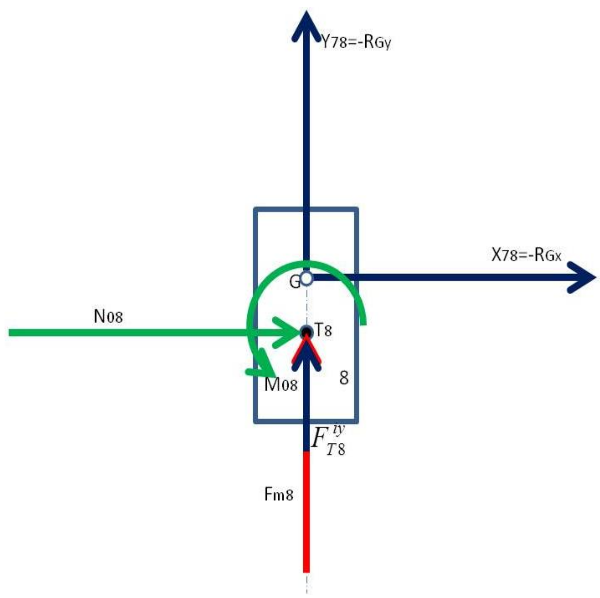

Fig. 8: Forces acting on the engine element 8

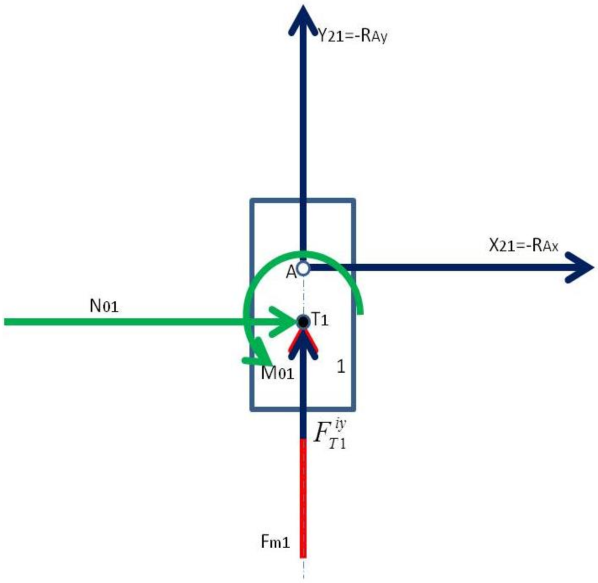

Fig. 9: Forces acting on the engine element 1

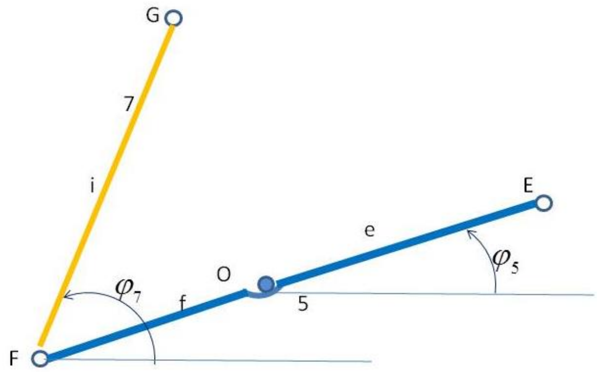

Fig. 10: Direct kinematics on dyad 5.7: Speeds and accelerations

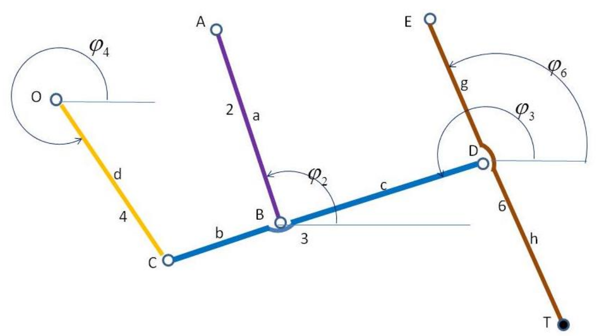

Fig. 11: Kinematics of the triad 2,3,4,6

Results and Discussion

Table 1 gives the input data, more precisely the known lengths of the mechanism (In the calculation program used these lengths represent the constant geometric parameters).

The point T located on the effector 6 (Fig. 1, 4-5) describes a rectangular trajectory (Fig. 12). Its characteristics are shown in Table 2.

The trajectory of the point T in Fig. 12 is described by the relationships in Table 3.

The coordinates represent the input parameters for the algorithm of the inverse positional model in Table 3.

Going through the connection of the modular groups for the inverse structural model (Fig. 2b, 3) the algorithm presented in Tables 2-3 allows the successive calculation of the dependent parameters (Fig. 4), as follows:

- for the dyad RRR (5,6) -Φ5k (XTk, YTk), Φ6k (XTk, YTk) can be seen in Fig. 13 [deg], as Φ50k (XTk, YTk), Φ60k (XTk, YTk)
- for the dyad RRR (3,4) -Φ3k (XTk, YTk), Φ4k (XTk, YTk) can be seen in the Fig. 14 [deg], as Φ30k (XTk, YTk), Φ40k (XTk, YTk)
- for dyad RRT (1,2) -Yak (XTk, YTk) and Φ2k (XTk, YTk) seen in Fig. 15, where
- Φ2k(XTk,YTk) in [deg] is Φ20k(XTk,YTk)
- for dyad RRT (8,7) -YGk (XTk, YTk) and Φ7k (XTk, YTk) seen in Fig. 16, where
- Φ7k (XTk, YTk) in [deg] is Φ70k (XTk, YTk)

It is considered a single external force (technological resistance) RTk that acts on the system neglecting other external forces (for example-gravitational forces) and the system of inertial forces. This simplification brings some peculiarities in the form of terms from the calculation algorithm without restricting its generality.

The external force RTk (Fig. 17) is considered constant on the initial and horizontal portion of the trajectory of the point T (Fig. 12) and is described by the relation (53):

$$RTk := if\left(k \le 10, 20, 0\right) \tag{53}$$

Using the connection of the modular groups for the direct structural model (Fig. 3) the passive module GMP2 (2,3,4,6), a 6R triad (Fig. 5, 6, 18) is analyzed in the first stage, for which elaborated algorithm, relations (1-20).

Applying the calculation algorithm (1-20) for the GMP2 triad (2,3,4,6) is determined reaction torsion components, as follows:

- In the kinematic torque of E → X56k, Y56k from Fig. 19
- In kinematic rotation couple from the point A → X12 k, Y12 k from Fig. 20

- In the kinematic rotation couple from the point B → X23 k = -X32 k, Y23 k = -Y32 k
- In the kinematic rotation couple from the point C → X43 k = -X34 k, Y43 k = -Y34 k
- In the kinematic rotation couple from the point D → X63 k = -X36 k, Y63 k = -Y36 k
- In the kinematic rotation couple from the point O → X04 k, Y04 k from Fig. 21

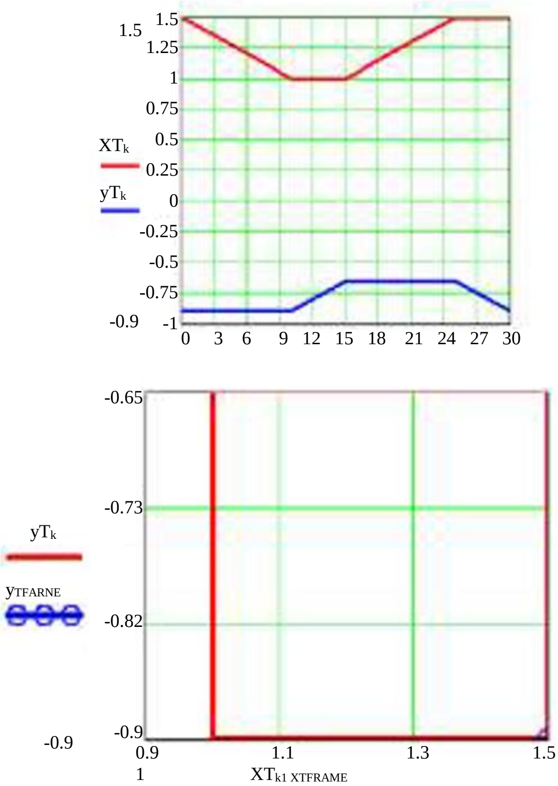

Fig. 12: The trajectory of the T-point, the end effector

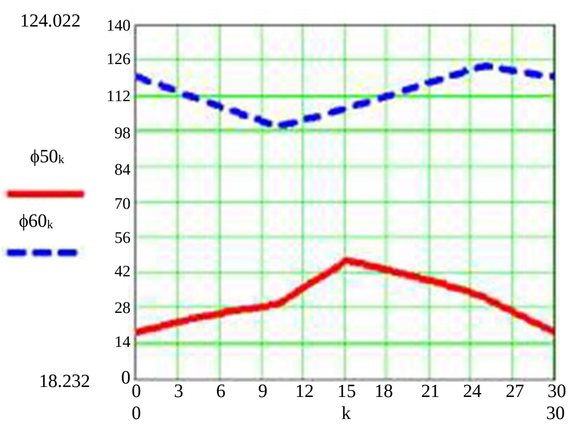

Fig. 13: Variation of angles FI5 and FI6 considered in [deg] depending on the independent parameter k

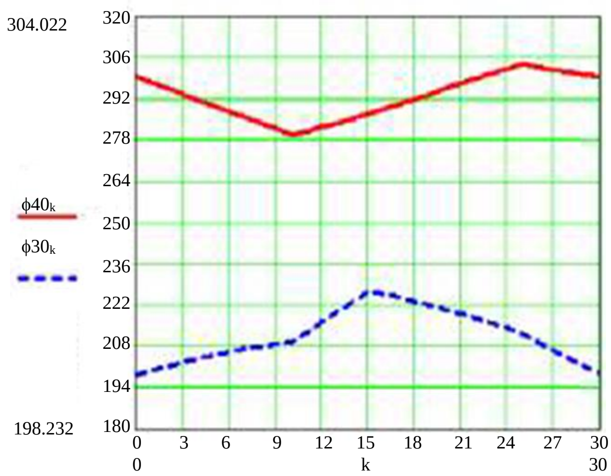

Fig. 14: Variation of angles FI3 and FI4 considered in [deg] depending on the independent parameter k

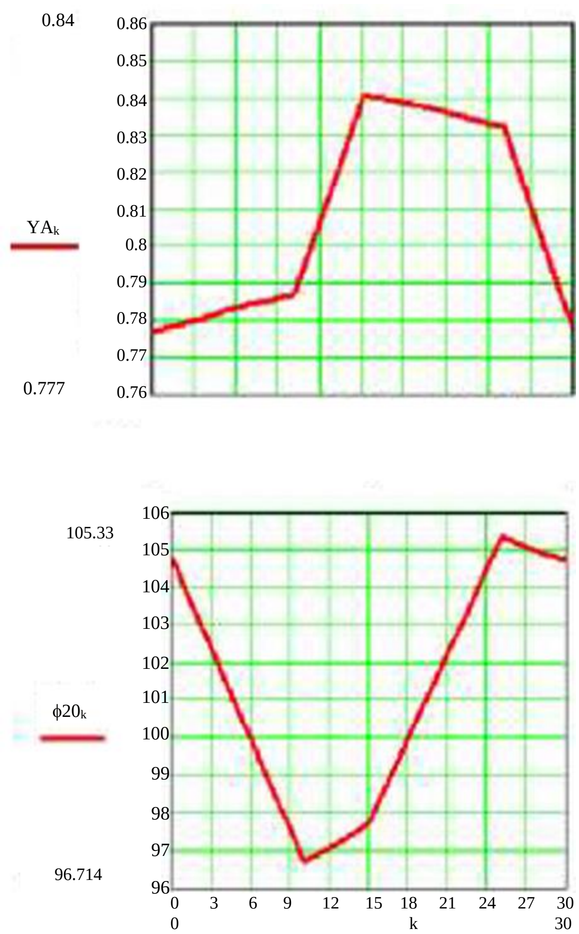

Fig. 15: The variation of the parameter YA and the angle FI2 considered in [deg] depending on the independent parameter k

DOI: 10.3844/ajeassp.2022.59.80

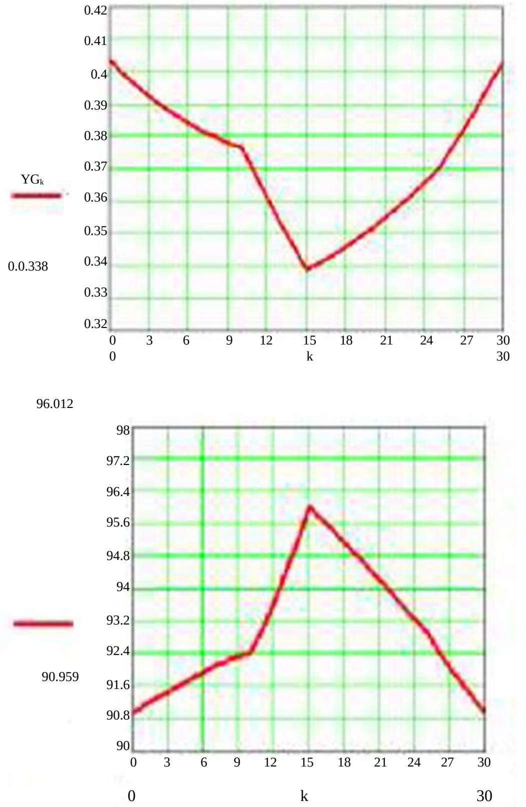

Fig. 16: Variation of parameter YG and angle FI7 considered in [deg] depending on the independent parameter k

Fig. 17: The external force RTk is considered constant on the initial and horizontal portion of the trajectory of the point T

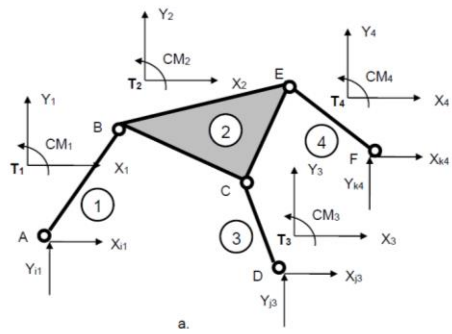

Fig. 18: Passive module GMP2 (2,3,4,6), the triad 6R

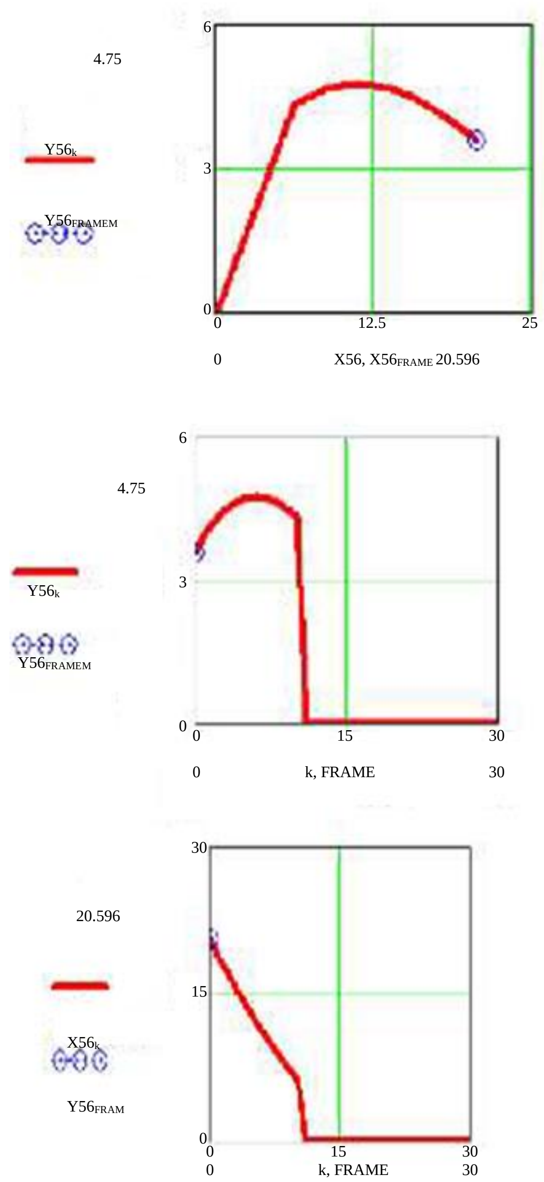

Fig. 19: Reaction torque in the kinematic rotation coupling of E $\rightarrow$ X56 k, Y56 k on the GMP 2 modular group (2,3,4,6), triad type 6 R

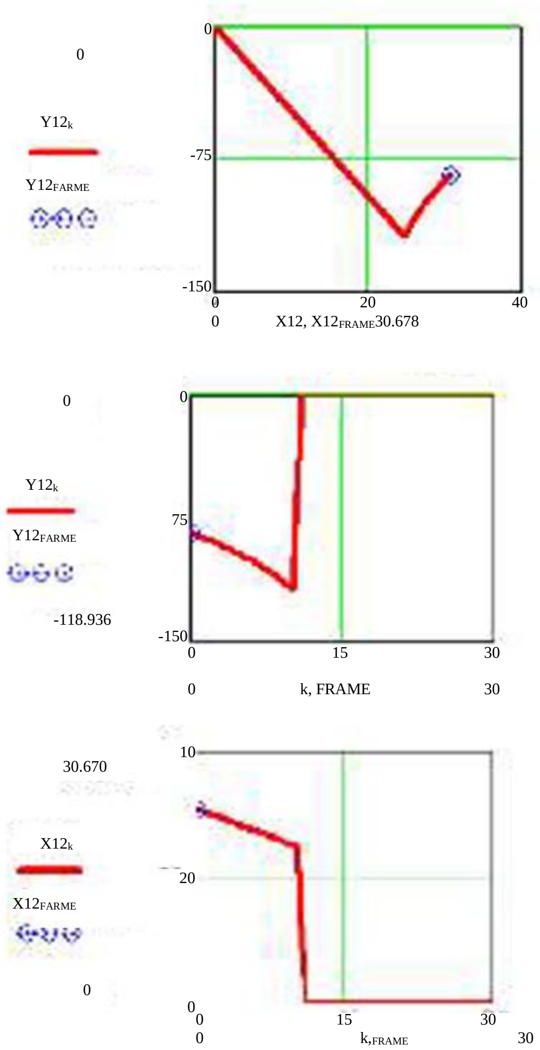

Fig. 20: Reaction torque in the kinematic torque of A → X12 k, Y12 k on the GMP 2 modular group (2,3,4,6), 6 R triad type

The next module in the modular group connection of the direct structural model (Fig. 7) is GMP1 (7.5) shown in Fig. 22 a, b, an RRR dyad for which the kinetostatic model is rendered by the relations (21-32).

In this calculation stage it is determined:

- In the kinematic torque from E → X87 k, Y87 k from Fig. 23
- In the kinematic rotation couple from the point O → X05k, Y05k from Fig. 24

In the following steps, the initial active modular groups GMAI (G, 8) and GMAI (A, 1) are shown in Fig. 25 a, b.

The components (NO8 k, T08 k) of the active translation coupling G are shown in Fig. 26 and for the active coupling of A (NO1k, T01k) in Fig. 27.

This bimobile 2T9R mechanism (Fig. 1) can be used by the simultaneous action of active translation torques in A and G point T having a chosen trajectory and law of motion. If one of these active couplings is locked, the mechanism remains with only one degree of mobility. The connections of the modular groups are given in both cases: Respectively, for G blocked and for A blocked in Fig. 28 a, b.

Applying the calculation modules, it is possible to study the behavior of the mechanism with a degree of mobility in the mentioned situations. Thus, if the active coupling G is blocked, the variation of the dependent parameters of the resulting mechanism is studied, with a degree of mobility (Fig. 29) for the extreme blocking positions Φ50 minimum and Φ50 maximum.

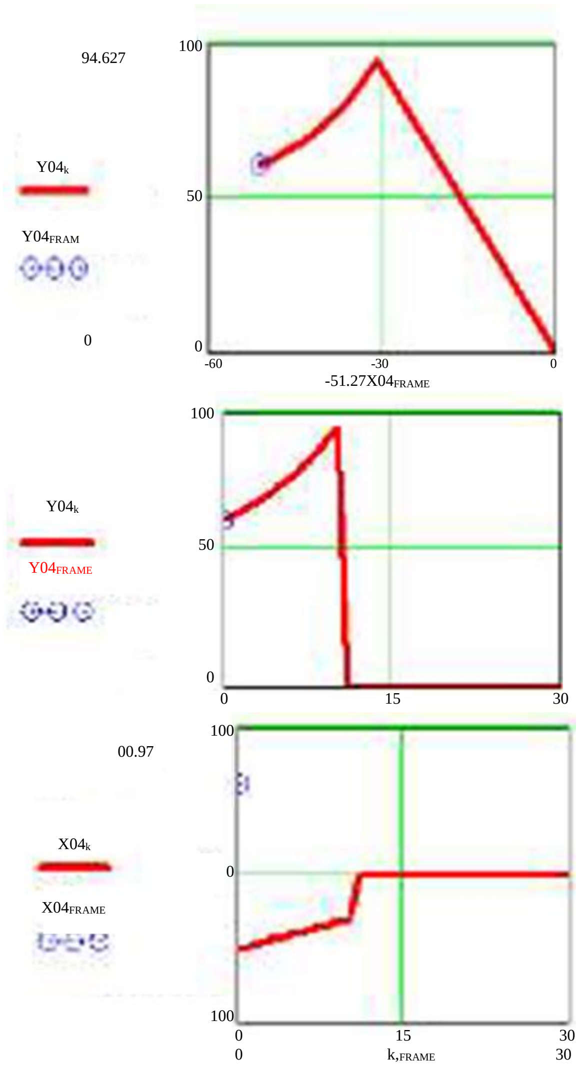

Fig. 21: Reaction torsion in the kinematic torque of O → X04 k, Y04 k on the GMP 2 modular group (2,3,4,6), triad type 6R

DOI: 10.3844/ajeassp.2022.59.80

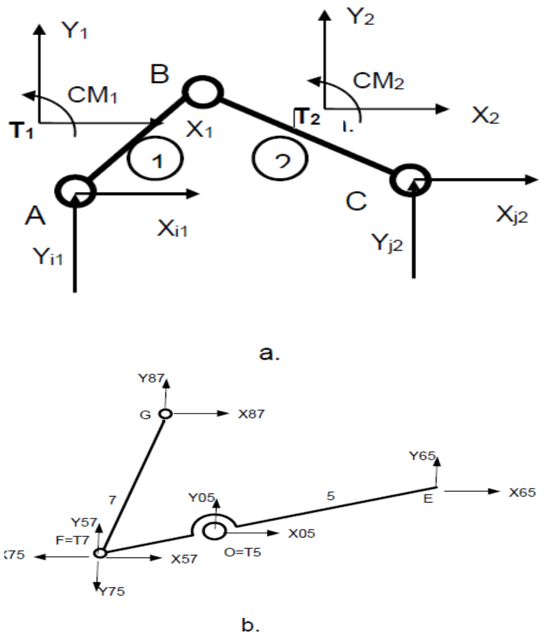

Fig. 22: Reaction torsor on the GMP1 dyad modular group (7.5)

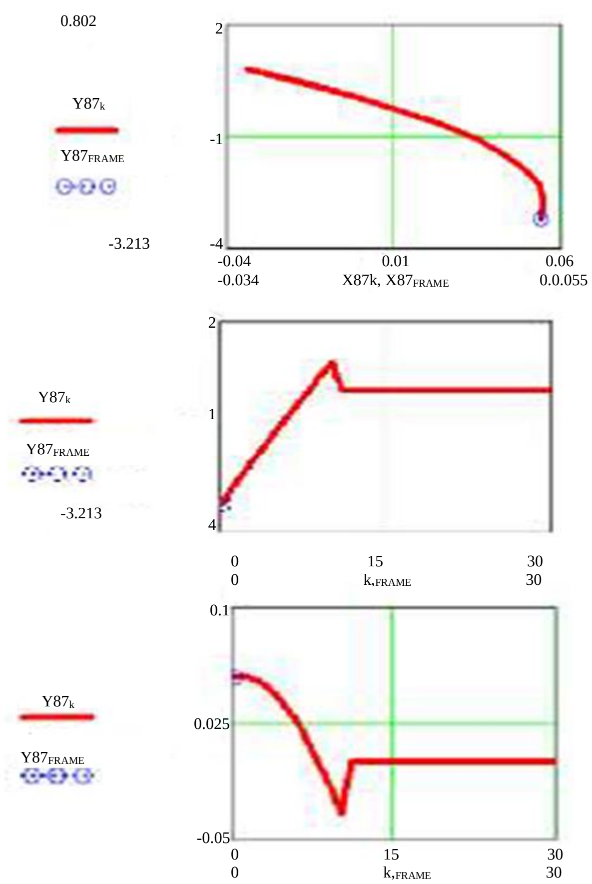

Fig. 23: Reaction torsor in kinematic coupling E, → X87 k, Y87 k, on the GMP 1 dyad modular group (7.5)

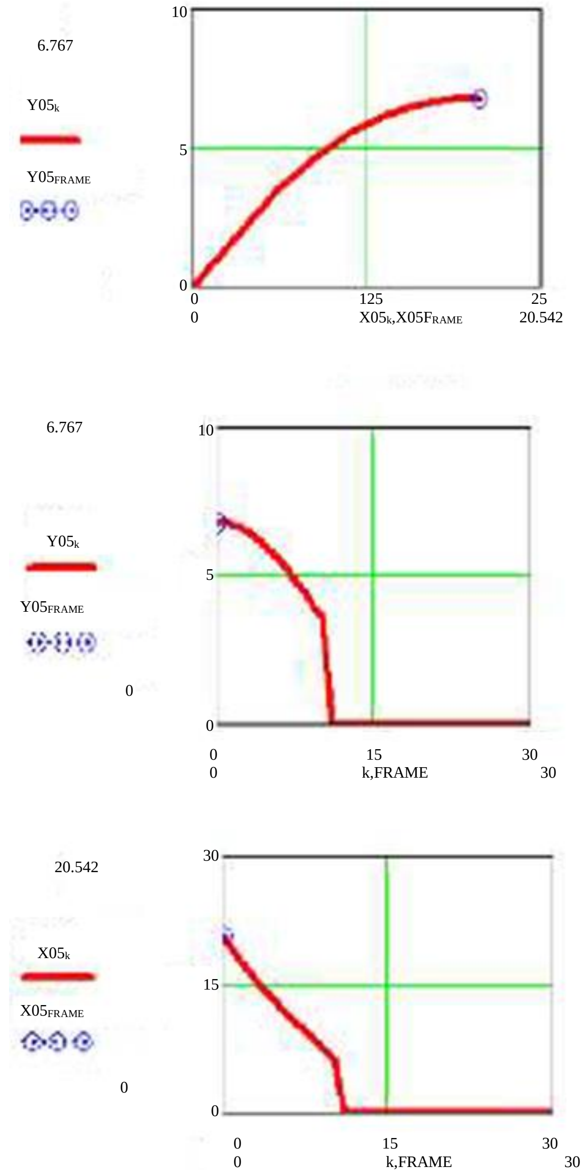

Fig. 24: Reaction torsor in kinematic coupling O, → X05 k, Y05 k, from the GMP 1 dyad modular group (7.5)

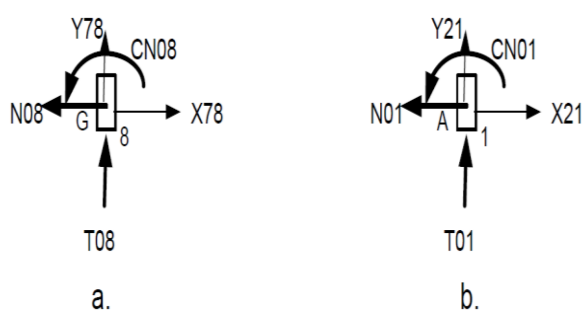

Fig. 25: The reaction torsor of the initial active modular groups GMAI (G, 8) a and GMAI (A, 1) b

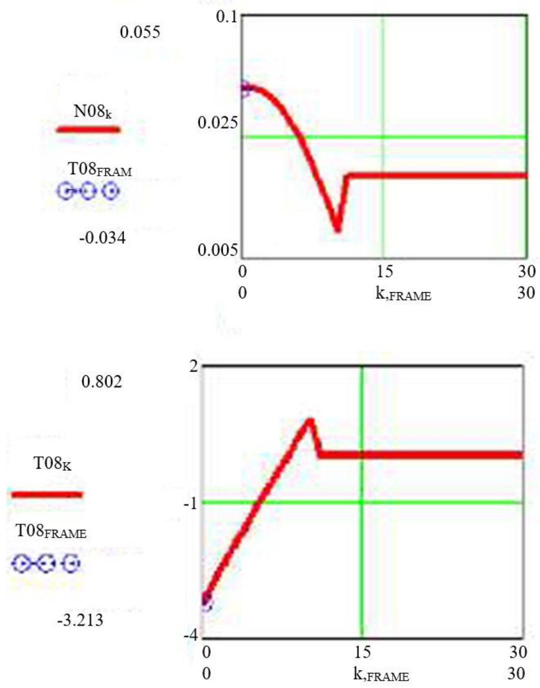

Fig. 26: Reaction torsor from the initial active modular group GMAI (G, 8)

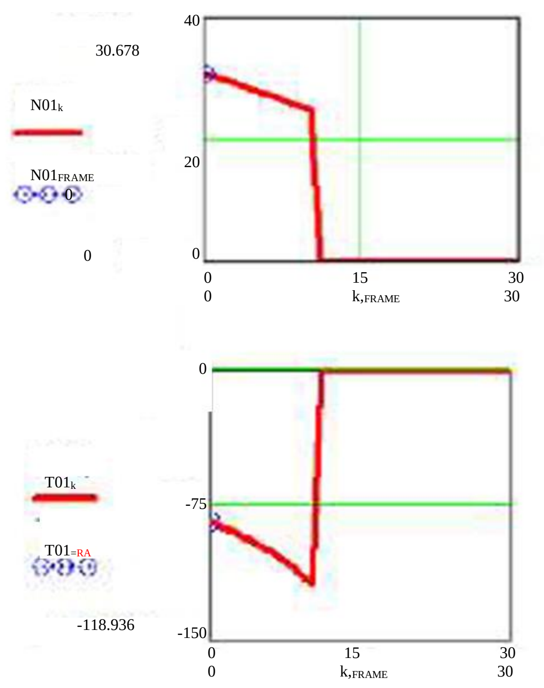

Fig. 27: Reaction torsor from the initial active modular group GMAI (A,1)

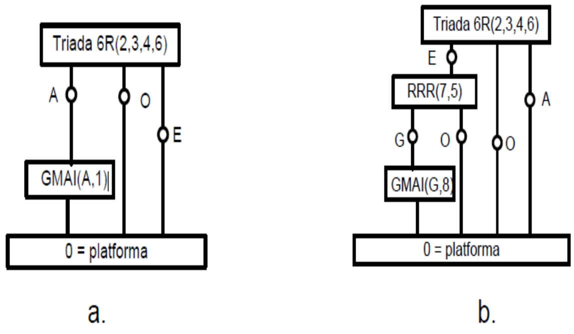

Fig. 28: The connections of the modular groups for the two distinct situations when G is blocked and the case when A is blocked, respectively

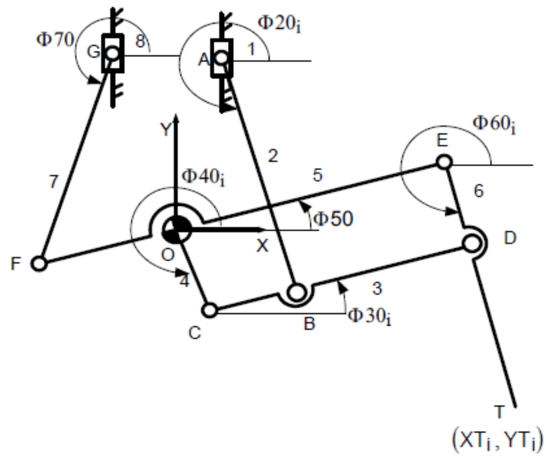

Fig. 29: The case in which the active coupling G is blocked when studying the variation of the dependent parameters of the resulting mechanism, with a degree of mobility for the extreme locking positions Φ 50 minimum and Φ 50 maximum

Table 1: Constant geometric parameters

XA	0.1	ET	1.35
XG	-0.15	OF	0.15
AB	1.15	FG	0.45
CD	0.88	TD	0.90
OE	0.88	BD	0.70
OC	0.45	BC	0.18
ED	0.45		

Table 2: Initial parameters of the T point trajectory

Initial parameters of the T point	T0 (1.5, -0.9)
The step of moving the T point horizontally - v	-0.05
The step of moving the T point vertically - v1	0.05

Table 3: The input parameters

Point T coordinates	*XTk =if [k ≤10, XT0 + kv, if [10< k≤ 15, XT0+ 10v, if[15<k ≤25,XT0 +10v- (k-15)v,XT0]]]* *YTk=if [k ≤10, YT0, if[10<k≤15,YT0 +(k- 10)v1, if [15< k ≤25, YT0 + 5v1, YT0 +5v1- (k – 25)v1]]]*

Conclusion

The kinematic and kinetostatic modeling of a 2T9R robotic mechanism is generally quite difficult and lucrative, but it has the advantages of obtaining a well-developed theoretical model that can be used in practice to design or use such robots, extremely interesting and useful, which has increased maneuverability, a large workspace, a correct and fast dynamics of movement, without vibrations or noises, the mechatronic module presented can be designed and built-in various ways depending on the requirements and objectives of the workplace in which it will be implemented.

The paper presented the inverse and direct kinematic models, the kinetostatic (forces) model that is always studied inversely, together with the related calculation relations.

In the results and discussions section, the diagrams obtained by calculation using the Math Cad 2000 program were presented.

Acknowledgment

This text was acknowledged and appreciated by Dr. Veturia CHIROIU Honorific member of the Technical Sciences Academy of Romania (ASTR) Ph.D. supervisor in Mechanical Engineering.

Funding Information

Research contract: Contract number 36-5-4D/1986 from 24IV1985, beneficiary CNST RO (Romanian National Center for Science and Technology) Improving dynamic mechanisms of internal combustion engines.

Author's Contributions

All the authors contributed equally to preparing, developing, and carrying out this manuscript.

Ethics

This article is original and contains unpublished material. The author declares that are no ethical issues and no conflict of interest that may arise after the publication of this manuscript.

References

Anderson, S. B. (1997). Historical Overview of V/STOL Aircraft Technology. NTRS-NASA Technical Reports Server. https://ntrs.nasa.gov/citations/20020051099

Antonescu, P., & Petrescu, F. (1985). Analytical method of synthesis of cam mechanism and flat stick. In Proceedings of the 4th International Symposium on Theory and Practice of Mechanisms, (TPM'89), Bucharest.

Antonescu, P., & Petrescu, F. (1989). Contributions to cinetoelastodynamic analysis of distribution mechanisms.

Antonescu, P., Oprean, M., & Petrescu, F. (1985a). Contributions to the synthesis of oscillating cam mechanism and oscillating flat stick. In Proceedings of the 4th International Symposium on Theory and Practice of Mechanisms, (TPM'85), Bucharest.

Antonescu, P., Oprean, M., & Petrescu, F. (1985b). At the projection of the oscillate cams, there are mechanisms and distribution variables. In Proceedings of the V-Conference for Engines, Automobiles, Tractors and Agricultural Machines, I-Engines and Automobiles, (AMA'85), Brasov.

Antonescu, P., Oprean, M., & Petrescu, F. (1986). Projection of the profile of the rotating camshaft acting on the oscillating plate with disengagement. In Proceedings of the 3rd National Computer-aided Design Symposium in the field of Mechanisms and Machine Parts, (MMP'86), Brasov.

Antonescu, P., Oprean, M., & Petrescu, F. (1987). Dynamic analysis of the cam distribution mechanisms. In Proceedings of the 7th National Symposium on Industrial Robots and Space Mechanisms, (RSM'87), Bucharest.

Antonescu, P., Oprean, M., & Petrescu, F. (1988). Analytical synthesis of Kurz profile, rotating the flat cam. Mach, Build. Rev.

Antonescu, P., Petrescu, F., & Antonescu, D. (1997). Geometrical synthesis of the rotary cam and balance tappet mechanism. Bucharest, 3, 23-23.

Antonescu, P., Petrescu, F., & Antonescu, O. (1994). Contributions to the synthesis of the rotating cam mechanism and the tip of the balancing tip.

Antonescu, P., Petrescu, F., & Antonescu, O. (2000a). Contributions to the synthesis of the rotary disc-cam profile. In Proceedings of the 8th International Conference on the Theory of Machines and Mechanisms, (TMM'00), Liberec, Czech Republic (pp. 51-56).

Antonescu, P., Petrescu, F., & Antonescu, O. (2000b). Synthesis of the rotary cam profile with balance follower. In Proceedings of the 8th Symposium on Mechanisms and Mechanical Transmissions, (MMT'00), Timişoara (pp. 39-44).

Antonescu, P., Petrescu, F., & Antonescu, O. (2001). Contributions to the synthesis of mechanisms with rotary disc-cam. In Proceedings of the 8th IFToMM International Symposium on Theory of Machines and Mechanisms, (TMM'01), Bucharest, ROMANIA (pp. 31-36).

Aversa, R., Petrescu, F. I., Petrescu, R. V., & Apicella, A. (2016a). Biomimetic finite element analysis bone modeling for customized hybrid biological prostheses development. American Journal of Applied Sciences, 13(11), 1060-1067.

Aversa, R., Parcesepe, D., Petrescu, R. V. V., Chen, G., Petrescu, F. I. T., Tamburrino, F., & Apicella, A. (2016b). Glassy amorphous metal injection molded induced morphological defects.

Aversa, R., Petrescu, R. V., Petrescu, F. I., & Apicella, A. (2016c). Smart-factory: Optimization and process control of composite centrifuged pipes. American Journal of Applied Sciences, 13(11), 1330-1341.

Aversa, R., Tamburrino, F., Petrescu, R. V., Petrescu, F. I., Artur, M., Chen, G., & Apicella, A. (2016d). Biomechanically inspired shape memory effect machines driven by muscle-like acting NiTi alloys. American Journal of Applied Sciences, 13(11), 1264-1271.

Aversa, R., Petrescu, R. V., Apicella, A., & Petrescu, F. I. (2017a). Nano-diamond hybrid materials for structural biomedical application. American Journal of Biochemistry and Biotechnology, 13(1), 34-41.

Aversa, R., Petrescu, R. V., Akash, B., Bucinell, R., Corchado, J., Chen, G., & Petrescu, F. I. (2017b). Kinematics and forces to a new model forging manipulator. American Journal of Applied Sciences, 14(1), 60-80.

Aversa, R., Petrescu, R. V., Apicella, A., Petrescu, F. I., Calautit, J. K., Bucinell, R., & Akash, B. (2017c). Something about the V engines design. American Journal of Applied Sciences, 14(1), 34-52.

Aversa, R., Parcesepe, D., Petrescu, R. V., Berto, F., Chen, G., Petrescu, F. I., & Apicella, A. (2017d). Process ability of bulk metallic glasses. American Journal of Applied Sciences, 14(2), 294-301.

Ayiei, A. (2020). The Use of Eye Tracking in Assessing Visual Attention. Journal of Aircraft and Spacecraft Technology. 4, 117-124. doi.org/10.3844/jastsp.2020.117.124

Babu, K. V., Rao, A. S., Kumar, K. N., & Rao, M. V. (2019). Spectral and luminescence properties of manganese doped sodium lead alumino borosilicate glass system. Journal of Aircraft and Spacecraft Technology, 3(1), 248-255. doi.org/10.3844/jastsp.2019.248.255

Babu, K. V., Subba Rao, A., Madhuri, V., & Suresh, K. (2020). White light generation in Dy3+-doped sodium leads to alumino borosilicate glasses for W-LED applications. Journal of Aircraft and Spacecraft Technology. 4(1), 39-47. doi.org/10.3844/jastsp.2020.39.47

Brewer, G. D. (1991). Hydrogen aircraft technology. CRC press.

Brischetto, S., & Torre, R. (2020). Honeycomb Sandwich Specimens Made of PLA and Produced Via 3D FDM Printing Process: An Experimental Study.

Cao, W., Ding, H., Zi, B., & Chen, Z. (2013). New structural representation and digital-analysis platform for symmetrical parallel mechanisms. International Journal of Advanced Robotic Systems, 10(5), 243. doi.org/10.5772/56380

Chaudhary, S., & Kumar, A. (2019). Control of twin rotor MIMO system using PID and LQR controller. Journal of Aircraft and Spacecraft Technology, 3(1), 211-220. doi.org/10.3844/jastsp.2019.211.220

Chilukuri, D., Yi, S., & Seong, Y. (2019). Computer Vision for Vulnerable Road Users using Machine Learning. Journal of Mechatronics and Robotics. 3, 33-41. doi.org/10.3844/jmrsp.2019.33.41

CEUP. (2018). Drone: Aviation safety reform in the EU. https://www.consilium.europa.eu/ro/policies/drones/

de Lima, M. S. F., de Mota Siqueira, R. H., de Carvalho, S. M., & Abdalla, A. J. (2019). Hardening Effects of In-Situ Aging for a Laser Welded Maraging Steel.

de Mota Siqueira, R. H., Atilio, I., de Andrade Ferreira, C. C., de Carvalho, S. M., & de Lima, M. S. F. (2020). Fiber Laser Beam Welding Between Niobium and Titanium. Journal of Aircraft and Spacecraft Technology. 4(1), 21-25. doi.org/10.3844/jastsp.2020.21.25

Dekkata, S. C., & S. Yi, (2019). Improved Steering and Adaptive Cruise Control for Autonomous Vehicles Using Model Predictive Control. Journal of Mechatronics and Robotics. 3, 378-388. doi.org/10.3844/jmrsp.2019.378.388

Dong, H., Giakoumidis, N., Figueroa, N., & Mavridis, N. (2013). Approaching behavior monitor and vibration indication in developing a General Moving Object Alarm System (GMOAS). International Journal of Advanced Robotic Systems, 10(7), 290. doi.org/10.5772/56586

Dwivedi, A., Kumar, D., & Tiwari, N. (2019a). A Review on Electric Traction using WE System.

Dwivedi, A., Rajbhar, P., & Tiwari, N. (2019b). Long Distance Power Transfer Technique: A Review.

Eissa, M. A., Darwish, R. R., & Bassiuny, A. M. (2019). New Model-Based Fault Detection Approach using Black Box Observer.

El Hassouni, B., Haddi, A., & Amrani, A. G. (2019). Critical Study of Several MPPT Techniques for Photovoltaic Systems. Journal of Mechatronics and Robotics. 3, 269-279. doi.org/10.3844/jmrsp.2019.269.279

Eremia, C. (2020). Has the era of air drone wars finally settled? Defense and Security Monitor. https://monitorulapararii.ro/epoca-razboaielor-dronelor-aeriene-s-a-instalat-definitiv-1-31794

Fahim, S. R., Dey, S., Rashiduzzaman, M., Sarker, S. K., Badal, F. R., & Das, S. K. (2019). Development of an Android Recognition Open-Loop Tracking Control of Writing Robotic Arm. Journal of Mechatronics and Robotics. 3, 521-533. doi.org/10.3844/jmrsp.2019.521.533

Franklin, D. J. (1930). Ingenious mechanisms for designers and inventors.

García, A. G. (2020). Asymptotic Stability of Unicycle-Like Robots: The Bessel’s Controller.

Garfo, S., Muktadir, M. A., & Yi, S. (2020). Defect Detection on 3D Print Products and in Concrete Structures Using Image Processing and Convolution Neural Network.

Hanrahan, J. (2014). Drone Attack Survival Guide could save your life. Vice Media Group. https://www.vice.com/ro/article/53p4xz/ghidul-de-supravietuire-a-atacurilor-cu-drone-ti-ar-putea-salva-viata

He, B., Wang, Z., Li, Q., Xie, H., & Shen, R. (2013). An analytic method for the kinematics and dynamics of a multiple-backbone continuum robot. International Journal of Advanced Robotic Systems, 10(1), 84. doi.org/10.5772/54051

Hertel, C. (2017). 10 questions you always wanted to ask a pilot. https://www.vice.com/ro/article/ne7va8/intrebari-pilot-curiozitati

Kisabo, A. B., & Adebimpe, A. F. (2019). State-Space Modeling of a Rocket for Optimal Control System Design. In Ballistics. IntechOpen. doi.org/10.5772/intechopen.82292

Kisabo, A. B., Adebimpe, A. F., & Samuel, S. O. (2019a). Pitch Control of a Rocket with a Novel LQG/LTR Control Algorithm.

Kisabo, A. B., Nwokolo, N., Adebimpe, A. F., & Samuel, S. O. (2019b). Novel Approach for Characterizing Solid Rocket Motor (SRM).

Komakula, S. A. (2019). Optimization of Inverse Kinematic Solution of a T4R Robotic Manipulator.

Kortam, M. A., Tolba, F. A., & Abdelkader Hassen, A. M. (2018). Development of a Mechatronic Control System for a Mechanical Fuel Injection System of a Four-Cylinder Automotive Diesel Engine by using Matlab and Simulink. Journal of Mechatronics and Robotics. 2, 60-71. doi.org/10.3844/jmrsp.2018.60.71

Kosambe, S. (2019a). NASA’s exploration missions to the red planet. Journal of Aircraft and Spacecraft Technology. 3(1), 154-171.

Kosambe, S. (2019b). Mission Shakti aka Project XSV-1: India’s First Anti-Satellite Test (ASAT).

Kosambe, S. (2019c). Overview of Space Debris Mitigation Activities in ISRO.

Kosambe, S. (2019d). Chandrayaan-2: India’s second lunar exploration mission. Journal of Aircraft and Spacecraft Technology, 3(1), 221-236.

Kumar, R. V. N., & Sreenivasulu, R. (2019). Inverse Kinematics (IK) Solution of a Robotic Manipulator using PYTHON. Journal of Mechatronics and Robotics. 3, 542-551. doi.org/10.3844/jmrsp.2019.542.551

Langston, L. S. (2015). Gas Turbines-Major Greenhouse Gas Inhibitors. Mechanical Engineering, 137(12), 54-55. doi.org/10.1115/1.2015-Nov-5

Langston, L. S. (2016). Hot Plates. Mechanical Engineering, 138(03), 42-47. doi.org/10.1115/1.2016-Mar-3

Lee, B. J. (2013). Geometrical derivation of differential kinematics to calibrate model parameters of flexible manipulator. International Journal of Advanced Robotic Systems, 10(2), 106. doi.org/10.5772/55592

Lin, W., Li, B., Yang, X., & Zhang, D. (2013). Modeling and control of inverse dynamics for a 5-DOF parallel kinematic polishing machine. International Journal of Advanced Robotic Systems, 10(8), 314. doi.org/10.5772/54966

Liu, H., Zhou, W., Lai, X., & Zhu, S. (2013). An efficient inverse kinematic algorithm for a PUMA560-structured robot manipulator. International Journal of Advanced Robotic Systems, 10(5), 236. doi.org/10.5772/56403

Matthews, M. T., & Yi, S. (2019). Adaptive and Neural Network Based Control of Pitch of Unmanned Aerial Vehicles.

Mishra, A. (2020a). Image Processing of Friction Stir Welded 6060-T5 Aluminum Alloy Joint.

Mishra, A. (2020b). Machine Learning Approach for Defects Identification in Dissimilar Friction Stir Welded Aluminium Alloys AA 7075-AA 1100 Joints.

Mishra, A., & Sarawagi, R. (2020). Local Binary Pattern for the Evaluation of Surface Quality of Dissimilar Friction Stir Welded Ultrafine Grained 1050 and 6061-T6 Aluminium Alloys. Journal of Mechatronics and Robotics. 4, 106-112. doi.org/10.3844/jmrsp.2020.106.112

Nacy, S. M., & Nayif, A. A. (2018). Effect of Object Size and Location on Contact Forces and Grasping Stability for an Underactuated Robotic Manipulator. Journal of Mechatronics and Robotics. 2, 72-84. doi.org/10.3844/jmrsp.2018.72.84

Oni, M. O., & Jha, B. K. (2019). Heat Generation/absorption effect on natural convection flow in a vertical annulus with time-periodic boundary conditions. Journal of Aircraft and Spacecraft Technology, 3(1), 183-196. doi.org/10.3844/jastsp.2019.183.196

Padula, F., & Perdereau, V. (2013). An online path planner for industrial manipulators. International Journal of Advanced Robotic Systems, 10(3), 156. doi.org/10.5772/55063

Perumaal, S. S., & Jawahar, N. (2013). Automated trajectory planner of industrial robot for pick-and-place task. International Journal of Advanced Robotic Systems, 10(2), 100. doi.org/10.5772/53940

Petrescu, F. I. T. (2012). Cold nuclear fusion. Plasma Phys. Fusion Technol. 44, 100-100.

Petrescu, F., & Petrescu, R. (2011a). Mechanical Systems, Serial and Parallel. Lulu. com.

Petrescu, F. I. T., & Petrescu, R. V. (2011b). Trenuri planetare. Createspace Independent Pub, 104.

Petrescu, F. I., & Petrescu, R. V. (2011c). Determination of the Mechanical Efficiency of the Gears. Ingineria Automobilului, (19), 22-23.

Petrescu, R. V. V. (2019a). Giant success for NASA when the in-sight probe has reached "safety" on Mars. Journal of Aircraft and Spacecraft Technology. 3(1), 1-10.

Petrescu, R. V. V. (2019b). Mars could have enough molecular oxygen to support life. Journal of Aircraft and Spacecraft Technology, 3(1), 11-23.

Petrescu, R. V. V. (2019c). About Boeing X-32. Journal of Aircraft and Spacecraft Technology, 3(1), 38-54.

Petrescu, R. V. V. (2019d). China Launches Its First Passenger Aircraft. Journal of Aircraft and Spacecraft Technology, 3, 64-77.

Petrescu, R. V. V. (2019e). NASA and the Conquest of Cosmic Space by Man. Journal of Aircraft and Spacecraft Technology, 3, 78-91.

Petrescu, R. V. V. (2019f). 'Defiant', A Today Unique Helicopter in the World. Journal of Aircraft and Spacecraft Technology, 3, 92-106.

Petrescu, R. V. V. (2019g). The TESS Satellite Will Search for Planets in the Vicinity of Our Solar System. Journal of Aircraft and Spacecraft Technology, 3, 107-118.

Petrescu, R. V. V. (2019h). Boeing's Autonomous Military Aircraft. Journal of Aircraft and Spacecraft Technology, 3, 138-153.

Petrescu, F. I. T. (2019i). About the nuclear particles' structure and dimensions. Computational Particle Mechanics, 6(2), 191-194.

Petrescu, R. V. (2019j). About the space robots. Journal of Mechatronics and Robotics, 3, 1-32. doi.org/10.3844/jmrsp.2019.1.32

Petrescu, R. V. (2019k). Medical service of robots. Journal of Mechatronics and Robotics, 3, 60-81.

Petrescu, R. V. (2019l). Dynamics at classical distribution. Journal of Mechatronics and Robotics, 3, 82-101.

Petrescu, R. V. (2019m). Time Factory. Journal of Mechatronics and Robotics, 3, 102-121.

Petrescu, R. V. (2019n). About robotics, mechatronics, and automation that help us Conquer the Cosmic Space. Journal of Mechatronics and Robotics, 3, 129-155.

Petrescu, R. V. (2019o). Dynamic models for rigid memory mechanisms. Journal of Mechatronics and Robotics, 3, 156-183.

Petrescu, R. V. (2019p). Something about a rail-bound forging manipulator. Journal of Mechatronics and Robotics, 3, 184-207.

Petrescu, R. V. (2019q). Face recognition as a biometric application. Journal of Mechatronics and Robotics, 3, 237-257.

Petrescu, R. V. (2019r). Contributions to the synthesis of fixed axle gears by avoiding the interference phenomenon. Journal of Mechatronics and Robotics, 3, 280-300.

Petrescu, R. V. (2019s). Space probes. Journal of Mechatronics and Robotics, 3, 301-343.

Petrescu, R. V. (2019t). Presents some aspects and applications of projective geometry. Available at SSRN 3445158.

Petrescu, R. V. (2019u). Mechanisms with rigid memory. Journal of Mechatronics and Robotics, 3, 431-470.

Petrescu, R. V. (2019v). Internal combustion engine forces. Journal of Mechatronics and Robotics, 3, 497-520.

Petrescu, F. I., & Petrescu, R. V. (2013a). Cinematics of the 3R Dyad.

Petrescu, F. I., & Petrescu, R. V. (2013b). Cams with high efficiency. Int. Rev. Mech. Eng, 7(4), 599-606.

Petrescu, F. I. T., & Petrescu, R. V. (2013c). An algorithm for setting the dynamic parameters of the classic distribution mechanism. Int. Rev. Modell. Simulat, 6, 1637-1641.

Petrescu, F. I., & Petrescu, R. V. (2013d). Dynamic synthesis of the rotary cam and translated tappet with a roll. Engevista, 15(3).

Petrescu, F. I., & Petrescu, R. V. (2013e). Forces and efficiency of cams. Int. Rev. Mech. Eng, 7(3), 507-511.

Petrescu, F. I. T., & Petrescu, R. V. V. (2014a). High-efficiency gear. Facta Universitatis, Series: Mechanical Engineering, 12(1), 51-60.

Petrescu, F. I., & Petrescu, R. V. (2014b). Cam gears dynamics in the classic distribution. Independent Journal of Management & Production (IJM&P), 5(1).

Petrescu, F. I., & Petrescu, R. V. (2014c). High-efficiency gears synthesis by avoiding the interferences. Independent Journal of Management & Production (IJM&P), 5(2).

Petrescu, F. I. T., & Petrescu, R. V. (2014d). Balancing otto engines. Int. Rev. Mech. Eng, 8, 473-480.

Petrescu, F. I. T., & Petrescu, R. V. (2014e). Machine equations to the classical distribution. Int. Rev. Mech. Eng, 8, 309-316.

Petrescu, F. I. T., & Petrescu, R. V. (2014f). Forces of internal combustion heat engines. Int. Rev. Modell. Simulat, 7, 206-212.

Petrescu, F. I. T., & Petrescu, R. V. (2014g). Determination of the yield of internal combustion thermal engines. Int. Rev. Mech. Eng, 8, 62-67.

Petrescu, F. I., & Petrescu, R. V. (2014h). Cam Dynamic Synthesis. Al-Khwarizmi Engineering Journal, 10(1), 1-23.

Petrescu, F. I. T., & Petrescu, R. V. V. (2019a). An algorithm to determine the gear efficiency of a simple planetary train. Independent Journal of Management & Production, 10(5), 1392-1404.

Petrescu, R. V., & Petrescu, F. I. (2019b). Structural-topological synthesis of space Mechanisms with rods and wheels. Independent Journal of Management & Production (IJM&P) v, 10.

Petrescu, F. I. T., & Petrescu, R. V. V. (2019c). Application to rigid memory mechanisms of a variable internal dynamic damping model. Independent Journal of Management AND Production, 10(6), 1994-2022.

Petrescu, N., & Petrescu, F. I. (2019d). The yield of the thermal engines. Journal of Mechatronics and Robotics, 3, 215-236.

Petrescu, N., & Petrescu, F. I. (2019e). Machine motion equations are presented in a new general format. Journal of Mechatronics and Robotics, 3, 344-377.

Petrescu, N., & Petrescu, F. I. (2019f). New about the balancing of thermal motors. Available at SSRN 3445153.

Petrescu, R. V., Aversa, R., Akash, B., Bucinell, R., Corchado, J., Apicella, A., & Petrescu, F. I. (2017a). Modern propulsions for aerospace-a review. Journal of Aircraft and Spacecraft Technology, 1(1).

Petrescu, R. V., Aversa, R., Akash, B., Bucinell, R., Corchado, J., Apicella, A., & Petrescu, F. I. (2017b). Modern propulsions for aerospace-part II. Journal of Aircraft and Spacecraft Technology, 1(1).

Petrescu, R. V., Aversa, R., Akash, B., Bucinell, R., Corchado, J., Apicella, A., & Petrescu, F. I. (2017c). History of an aviation-a short review. Journal of Aircraft and Spacecraft Technology, 1(1).

Petrescu, R. V., Aversa, R., Akash, B., Bucinell, R., Corchado, J., Apicella, A., & Petrescu, F. I. (2017d). Lockheed martin-a short review. Journal of Aircraft and Spacecraft Technology, 1(1).

Petrescu, R. V., Aversa, R., Akash, B., Corchado, J., Apicella, A., & Petrescu, F. I. (2017e). Our universe. Journal of Aircraft and Spacecraft Technology, 1(2).

Petrescu, R. V., Aversa, R., Akash, B., Corchado, J., Apicella, A., & Petrescu, F. I. (2017f). What is a UFO? Journal of Aircraft and Spacecraft Technology, 1(2).

Petrescu, R. V., Aversa, R., Akash, B., Corchado, J., Berto, F., Mirsayar, M., ... & Petrescu, F. I. T. (2017g). About bell helicopter FCX-001 concept aircraft-a short review. Journal of Aircraft and Spacecraft Technology, 1(2), 91-96.

Petrescu, R. V., Aversa, R., Akash, B., Corchado, J., Apicella, A., & Petrescu, F. I. (2017h). Home at airbus. Journal of Aircraft and Spacecraft Technology, 1(2).

Petrescu, R. V., Aversa, R., Akash, B., Corchado, J., Kozaitis, S., Abu-Lebdeh, T., ... & Petrescu, F. I. (2017i). Airlander. Journal of Aircraft and Spacecraft Technology, 1(2).

Petrescu, R. V., Aversa, R., Akash, B., Corchado, J., Berto, F., Apicella, A., & Petrescu, F. I. (2017j). When Boeing is dreaming–a review. Journal of Aircraft and Spacecraft Technology, 1(3).

Petrescu, R. V., Aversa, R., Akash, B., Corchado, J., Berto, F., Apicella, A., & Petrescu, F. I. (2017k). About Northrop Grumman. Journal of Aircraft and Spacecraft Technology, 1(3).

Petrescu, R. V., Aversa, R., Akash, B., Corchado, J., Berto, F., Apicella, A., & Petrescu, F. I. (2017l). Some special aircraft. Journal of Aircraft and Spacecraft Technology, 1(3).

Petrescu, R. V., Aversa, R., Akash, B., Corchado, J., Berto, F., Apicella, A., & Petrescu, F. I. (2017m). About helicopters. Journal of Aircraft and Spacecraft Technology, 1(3), 204-223.

Petrescu, R. V., Aversa, R., Akash, B., Berto, F., Apicella, A., & Petrescu, F. I. (2017n). The modern flight. Journal of Aircraft and Spacecraft Technology, 1(4), 224-233.

Petrescu, R. V., Aversa, R., Akash, B., Berto, F., Apicella, A., & Petrescu, F. I. (2017o). Sustainable energy for aerospace vessels. Journal of Aircraft and Spacecraft Technology, 1(4), 234-240.

Petrescu, R. V., Aversa, R., Akash, B., Berto, F., Apicella, A., & Petrescu, F. I. (2017p). Unmanned helicopters. Journal of Aircraft and Spacecraft Technology, 1(4), 241-248.

Petrescu, R. V., Aversa, R., Akash, B., Berto, F., Apicella, A., & Petrescu, F. I. (2017q). Project HARP. Journal of Aircraft and Spacecraft Technology, 1(4), 249-257.

Petrescu, R. V., Aversa, R., Akash, B., Berto, F., Apicella, A., & Petrescu, F. I. (2017r). Presentation of Romanian Engineers who Contributed to the Development of Global Aeronautics–Part I. Journal of Aircraft and Spacecraft Technology, 1(4), 258-271.

Petrescu, R. V., Aversa, R., Akash, B., Berto, F., Apicella, A., & Petrescu, F. I. (2017s). A first-class ticket to the planet mars, please. Journal of Aircraft and Spacecraft Technology, 1(4), 272-281.

Petrescu, R. V., Aversa, R., Li, S., Bucinell, R., Kozaitis, S., Abu-Lebdeh, T., & Petrescu, F. I. (2017s). Electron dimensions. American Journal of Engineering and Applied Sciences, 10(2), 584-602.

Petrescu, R. V., Aversa, R., Kozaitis, S., Apicella, A., & Petrescu, F. I. (2017u). Deuteron dimensions. American Journal of Engineering and Applied Sciences, 10(3).

Petrescu, R. V., Aversa, R., Kozaitis, S., Apicella, A., & Petrescu, F. I. (2017v). Some proposed solutions to achieve nuclear fusion. American Journal of Engineering and Applied Sciences, 10(3).

Petrescu, R. V., Aversa, R., Kozaitis, S., Apicella, A., & Petrescu, F. I. (2017w). Some basic reactions in nuclear fusion. American Journal of Engineering and Applied Sciences, 10(3).

Petrescu, F. I. T., Petrescu, R. V., & Mirsayar, M. (2017x). The computer algorithm for machine equations of classical distribution. Journal of Materials and Engineering Structures «JMES», 4(4), 193-209.

Petrescu, R. V., Aversa, R., Apicella, A., Kozaitis, S., Abu-Lebdeh, T., Akash, B., & Petrescu, F. I. (2017y). Triton for nuclear fusion. American Journal of Engineering and Applied Sciences, 10(4).

Petrescu, R. V., Aversa, R., Akash, B., Berto, F., Apicella, A., & Petrescu, F. I. (2017z). Forces of a 3R robot. Journal of Mechatronics and Robotics, 1(1).

Petrescu, R. V., Aversa, R., Akash, B., Berto, F., Apicella, A., & Petrescu, F. I. (2017aa). Direct geometry and cinematic to the MP-3R systems. Journal of Mechatronics and Robotics, 1(1).

Petrescu, R. V., Aversa, R., Akash, B., Berto, F., Apicella, A., & Petrescu, F. I. (2017ab). Dynamic elements at MP3R. Journal of Mechatronics and Robotics, 1(2), 24-37.

Petrescu, R. V., Aversa, R., Akash, B., Berto, F., Apicella, A., & Petrescu, F. I. (2017ac). Geometry and direct kinematics to MP3R with 4 × 4 operators. Journal of Mechatronics and Robotics, 1(2), 38-46.

Petrescu, R. V., Aversa, R., Apicella, A., Kozaitis, S., Abu-Lebdeh, T., & Petrescu, F. I. (2017ad). Current stage in the field of mechanisms with gears and rods. Journal of Mechatronics and Robotics, 1(2), 47-57.

Petrescu, R. V., Aversa, R., Apicella, A., Kozaitis, S., Abu-Lebdeh, T., & Petrescu, F. I. (2017ae). Geometry and inverse are kinematic at the MP3R mobile systems. Journal of Mechatronics and Robotics, 1(2), 58-65.

Petrescu, R. V., Aversa, R., Apicella, A., Kozaitis, S., Abu-Lebdeh, T., & Petrescu, F. I. (2017af). Synthesis of optimal trajectories with functions control at the level of the kinematic drive couplings. Journal of Mechatronics and Robotics, 1(2), 66-74.

Petrescu, R. V., Aversa, R., Apicella, A., Kozaitis, S., Abu-Lebdeh, T., & Petrescu, F. I. (2017ag). The inverse kinematics of the plane system 2-3 in a mechatronic MP2R system, by a trigonometric method. Journal of Mechatronics and Robotics, 1(2), 75-87.

Petrescu, R. V., Aversa, R., Apicella, A., Kozaitis, S., Abu-Lebdeh, T., & Petrescu, F. I. (2017ah). Serial, anthropomorphic, spatial, and mechatronic systems can be studied more simply in a plan. Journal of Mechatronics and Robotics, 1(2), 88-97.

Petrescu, R. V., Aversa, R., Apicella, A., Kozaitis, S., Abu-Lebdeh, T., & Petrescu, F. I. (2017ai). Analysis and synthesis of mechanisms with bars and gears used in robots and manipulators. Journal of Mechatronics and Robotics, 1(2), 98-108.

Petrescu, R. V., Aversa, R., Apicella, A., Kozaitis, S., Abu-Lebdeh, T., & Petrescu, F. I. (2017aj). Speeds and accelerations in direct kinematics to the MP3R systems. Journal of Mechatronics and Robotics, 1(2), 109-117.

Petrescu, R. V., Aversa, R., Apicella, A., Kozaitis, S., Abu-Lebdeh, T., & Petrescu, F. I. (2017ak). Geometry and determining the positions of a plan transporter manipulator. Journal of Mechatronics and Robotics, 1(2), 118-126.

Petrescu, F. I., & Calautit, J. K. (2016a). About nano fusion and dynamic fusion. American Journal of Applied Sciences, 13(3).

Petrescu, F. I., & Calautit, J. K. (2016b). About the light dimensions. American Journal of Applied Sciences, 13(3).

Petrescu, F. I., & Petrescu, R. V. (2005a). The cam is designed for better efficiency. SSRN 3076805.

Petrescu, F. I., & Petrescu, R. V. (2005b, September). Contributions to the Dynamic of Cams. In The Ninth IFTOMM International Symposium on Theory of Machines and Mechanisms.

Petrescu, F. I., & Petrescu, R. V. (2005c). Determining the dynamic efficiency of cams. Available at SSRN 3076802.

Petrescu, F. I., & Petrescu, R. V. (2005d). An original internal combustion engine. In The Ninth IFTOMM International Symposium on Theory of Machines and Mechanisms.

Petrescu, R. V., & Petrescu, F. I. (2005e). Determining the mechanical efficiency of the Otto engine's mechanism. SSRN 3076804.

Petrescu, F. I., & Petrescu, R. V. (2012a). Kinematics of the planar quadrilateral mechanism.

Petrescu, F. I., & Petrescu, R. V. (2012b). Mecatronica-sisteme seriale si paralele.

Petrescu, F. I., & Petrescu, R. V. (2016a). Parallel moving mechanical systems kinematics.

Petrescu, F. I., & Petrescu, R. V. (2016b). Direct and inverse kinematics to the anthropomorphic robots.

Petrescu, F. I., & Petrescu, R. V. (2016c). Dynamic cinematic to a structure 2R. GEINTEC Journal, 6(2).

Petrescu, F. I., Apicella, A., Petrescu, R. V., Kozaitis, S., Bucinell, R., Aversa, R., & Abu-Lebdeh, T. (2016). Environmental protection through nuclear energy. American Journal of Applied Sciences, 13(9), 941-946. doi.org/10.3844/ajassp.2016.941.946

Petrescu, F. I., Grecu, B., Comanescu, A., & Petrescu, R. V. (2009, October). Some mechanical design elements. In The 3rd International Conference on Computational Mechanics and Virtual Engineering COMEC (pp. 29-30).

Petrescu, F., & Petrescu, R. (1995a). Contributions to optimization of the polynomial motion laws of the stick from the internal combustion engine distribution mechanism. Bucharest, 1, 249-256.

Petrescu, F., & Petrescu, R. (1995b). Contributions to the synthesis of internal combustion engine distribution mechanisms. Bucharest, 1, 257-264.

Petrescu, F., & Petrescu, R. (1997a). Dynamics of cam mechanisms (exemplified on the classic distribution mechanism). Bucharest, 3, 353-358.

Petrescu, F., & Petrescu, R. (1997b). Contributions to the synthesis of the distribution mechanisms of internal combustion engines with a Cartesian coordinate method. Bucharest, 3, 359-364.

Petrescu, F., & Petrescu, R. (1997c). Contributions to maximizing polynomial laws for the active stroke of the distribution mechanism from internal combustion engines. Bucharest, 3, 365-370.

Petrescu, F., & Petrescu, R. (2000a). Synthesis of distribution mechanisms by the rectangular (Cartesian) coordinate method. University of Craiova, Craiova.

Petrescu, F., & Petrescu, R. (2000b). The design (synthesis) of cams using the polar coordinate method (triangle method). University of Craiova, Craiova.

Petrescu, F., & Petrescu, R. (2002a). Motion laws for cams. In Proceedings of the International Computer Assisted Design, National Symposium with Participation,(SNP'02), Braşov (pp. 321-326).

Petrescu, F., & Petrescu, R. (2002b). Camshaft dynamics elements. In Proceedings of the International Computer Assisted Design, National Participation Symposium, (SNP'02), Braşov (pp. 327-332).

Petrescu, F., & Petrescu, R. (2003). Some elements regarding the improvement of the engine design. In Proceedings of the National Symposium, Descriptive Geometry, Technical Graphics and Design, (GTD'03), Braşov (pp. 353-358).

Petrescu, F. I. T., (2011). Teoria Mecanismelor si a Masinilor: Curs Si Aplicatii. 1st Edn., CreateSpace Independent Publishing Platform. ISBN-10: 1468015826. pp: 432.

Petrescu, R. V., Aversa, R., Apicella, A., & Petrescu, F. I. (2018a). Romanian Engineering'On the Wings of the Wind'. Journal of Aircraft and Spacecraft Technology, 2(1), 1-18.

Petrescu, R. V., Aversa, R., Apicella, A., & Petrescu, F. I. (2018b). NASA Data was used to discover the eighth planet circling a distant star. Journal of Aircraft and Spacecraft Technology, 2(1), 19-30.

Petrescu, R. V., Aversa, R., Apicella, A., & Petrescu, F. I. (2018c). NASA has found the most distant black hole. Journal of Aircraft and Spacecraft Technology, 2(1), 31-39.

Petrescu, R. V., Aversa, R., Apicella, A., & Petrescu, F. I. (2018d). Nasa selects concepts for a new mission to titan, the moon of Saturn. Journal of Aircraft and Spacecraft Technology, 2(1), 40-52.

Petrescu, R. V., Aversa, R., Apicella, A., & Petrescu, F. I. (2018e). NASA sees first in 2018 the direct proof of ozone hole recovery. Journal of Aircraft and Spacecraft Technology, 2(1), 53-64.

Petrescu, R. V., Aversa, R., Apicella, A., & Petrescu, F. I. (2018f). An Exoplanet has Smothering Stratosphere without Water. Relly Victoria Petrescu *et al*./Journal of Aircraft and Spacecraft Technology, 2, 65-71.

Petrescu, R. V., Aversa, R., Apicella, A., & Petrescu, F. I. (2018g). Structure of Buried Ice on Mars. Relly Victoria Petrescu *et al*./Journal of Aircraft and Spacecraft Technology, 2, 72-79.

Petrescu, N., Aversa, R., Apicella, A., & Petrescu, F. I. (2018h). A New Exoplanet Reveals its Identity. Nicolae Petrescu *et al*./Journal of Aircraft and Spacecraft Technology, 2, 85-96.

Petrescu, N., Aversa, R., Apicella, A., & Petrescu, F. I. (2018i). New Researches Examines the Wing Shapes to Reduce Vortex and Wake. Journal of Aircraft and Spacecraft Technology, 2, 97-110.

Petrescu, R. V., Aversa, R., Apicella, A., & Petrescu, F. I. (2018j). Romanian Engineering' On the Wings of the Wind'. Journal of Aircraft and Spacecraft Technology, 2(1), 1-18.

Petrescu, R. V., Aversa, R., Apicella, A., & Petrescu, F. I. (2018k). NASA Data was used to discover the eighth planet circling a distant star. Journal of Aircraft and Spacecraft Technology, 2(1), 19-30.

Petrescu, R. V., Aversa, R., Apicella, A., & Petrescu, F. I. (2018l). NASA has found the most distant black hole. Journal of Aircraft and Spacecraft Technology, 2(1), 31-39.

Petrescu, R. V., Aversa, R., Apicella, A., & Petrescu, F. I. (2018m). Nasa selects concepts for a new mission to titan, the moon of Saturn. Journal of Aircraft and Spacecraft Technology, 2(1), 40-52.

Petrescu, R. V., Aversa, R., Apicella, A., & Petrescu, F. I. (2018n). NASA sees first in 2018 the direct proof of ozone hole recovery. Journal of Aircraft and Spacecraft Technology, 2(1), 53-64.

Petrescu, R. V., Aversa, R., Apicella, A., & Petrescu, F. I. (2018o). Modern propulsions for the aerospace industry. American Journal of Engineering and Applied Sciences, 11(2), 715-755.

Petrescu, R. V., Aversa, R., Apicella, A., Kozaitis, S., Abu-Lebdeh, T., & Petrescu, F. I. (2018p). Inverse kinematics of a Stewart platform. Journal of Mechatronics and Robotics, 2(1), 45-59.

Petrescu, R. V., Aversa, R., Apicella, A., & Petrescu, F. I. (2018q). Total static balancing and kinetostatics of the 3R base cinematic Chain. Journal of Mechatronics and Robotics, 2(1), 1-13.

Petrescu, R. V., Aversa, R., Apicella, A., & Petrescu, F. I. (2018r). Switching from flat to spatial motion to 3R mechatronic systems. Journal of Mechatronics and Robotics, 2(1), 14-22.

Petrescu, R. V., Aversa, R., Apicella, A., & Petrescu, F. I. (2018s). The dynamics of the planar cinematic balanced chain at the plan module 3R. Journal of Mechatronics and Robotics, 2(1), 23-34.

Petrescu, R. V., Aversa, R., Apicella, A., & Petrescu, F. I. (2018t). Dynamic kinematics of the plan balanced chain at the planar module 3R. Journal of Mechatronics and Robotics, 2(1), 35-44.

Petrescu, R. V., Aversa, R., Apicella, A., Kozaitis, S., Abu-Lebdeh, T., & Petrescu, F. I. (2018u). Inverse kinematics of a Stewart platform. Journal of Mechatronics and Robotics, 2(1), 45-59.

Petrescu, N., Aversa, R., Apicella, A., & Petrescu, F. I. (2018v). Something about Robots Today. Journal of Mechatronics and Robotics, 2, 85-104.

Petrescu, N., Aversa, R., Apicella, A., & Petrescu, F. I. (2018w). Structural-Topological Synthesis of Planar Mechanisms with Rods and Wheels. Journal of Mechatronics and Robotics, 2, 105-120.

Petrescu, R. V. V. (2020a). British Airways is Ordering up to 42 Boeing 777-9s Aeronaves to Modernize the UK Flag Carriers Long-Haul Fleet.

Petrescu, R. V. V. (2020b). Presentation of Four-stroke Engine Design Elements. Journal of Mechatronics and Robotics, 4, 15-41.

Petrescu, R. V. V. (2020c). Presents the Kinematics and Forces at a Basic Anthropomorphic Robot. Journal of Mechatronics and Robotics, 4, 42-73.

Petrescu, R. V. V. (2020d). Presents the Kinematics of a Manipulator with Three Mobilities. Journal of Mechatronics and Robotics, 4, 85-105.

Petrescu, R. V. V. (2020e). Nanobotics. Journal of Mechatronics and Robotics, 4, 136-155.

Petrescu, R. V. V. (2020f). Mechatronic Systems to the Braking Mechanisms. Journal of Mechatronics and Robotics, 4, 156-190.

Petrescu, R. V. V. (2020g). Fishing for “16 Psyche”. Journal of Aircraft and Spacecraft Technology, 4, 136-151.

Petrescu, R. V. V., & Petrescu, F. I. T. (2020). About gateway. Journal of Aircraft and Spacecraft Technology. 4(1), 70-87. doi.org/10.3844/jastsp.2020.70.87

Petrescu, R. V. V., Aversa, R., & Apicella, A. (2020). Structural color from optical phenomena caused by interference with a thin or multilayer film, photonic nanocrystals, light scattering, and diffraction grating effect. Journal of Aircraft and Spacecraft Technology. 4(1), 117-143. doi.org/10.3844/jastsp.2020.117.143

Petrescu, R. V., Petrescu, F. I., & Popescu, N. (2007). Determining gear efficiency. Gear Solutions.

Rahman, Z. A. (2018). On a New Equation for the Design and Development of Space Launch Vehicles. Journal of Aircraft and Spacecraft Technology, 2(1), 80-84. doi.org/10.3844/jastsp.2018.80.84

Rana, S. (2020). Improved 3D Imaging Performance of AFM. Journal of Mechatronics and Robotics, 4, 8-14. doi.org/10.3844/jmrsp.2020.8.14

Richmond, B. (2013). Kristian von Bengtson, Space Mission. https://www.vice.com/ro/article/4xdb5g/prima-misiune-cu-pilot-pe-luna-lui-jupiter-va-fi-planificata-prin-crowdsourcing

Riman, C. F. (2018). Multi-Controlled Wheelchair for Upper Extremities Disability. Journal of Mechatronics and Robotics, 2, 121-131. doi.org/10.3844/jmrsp.2018.121.131

Riman, C. F. (2019). Cheap Bluetooth Solution for Smart Controlled Home Devices. Journal of Mechatronics and Robotics, 3, 589-595. doi.org/10.3844/jmrsp.2019.589.595

Saheed, A., Adeyinka, O. M., & Zulikha, A. B. (2019). Access Control, Fire Prevention, and Surveillance Security System. Journal of Mechatronics and Robotics, 3, 563-570. doi.org/10.3844/jmrsp.2019.563.570

Sharma, A., & Kosambe, S. (2020). Trajectory optimization for a first human asteroid exploration mission. Journal of Aircraft and Spacecraft Technology. 4(1), 96-116. doi.org/10.3844/jastsp.2020.96.116

Svensson, F., Hasselrot, A., & Moldanova, J. (2004). Reduced environmental impact by lowered cruise altitude for liquid hydrogen-fuelled aircraft. Aerospace Science and Technology, 8(4), 307-320. doi.org/10.1016/j.ast.2004.02.004

Tumino, D. (2020). Mathematical formulation and numerical implementation of a finite element with anisotropic geometry. Journal of Aircraft and Spacecraft Technology. 4(1), 26-38. doi.org/10.3844/jastsp.2020.26.38

Vladescu, I. (2020). The flying car exists. The US Air Force has successfully tested it. https://evz.ro/gata-masina-zburatoare-exista-us-air-force-a-testat-o-cu-succes.html?utm_source=onesignal&fbclid=IwAR3WWmFTIz_DBQAAwpWlDC3zsLJFaZ5KiKJsGx7vaiuCkx_2JTuOWn2YuSQ

Welabo, A., & Tesfamariamr, G. (2020). Trajectory Tracking Control of UR5 Robot Manipulator Using Fuzzy Gain Scheduling Terminal Sliding Mode Controller. Journal of Mechatronics and Robotics, 4, 113-135. doi.org/10.3844/jmrsp.2020.113.135

Welch, H., & Mondal, S. (2019). Analysis of Magnetic Wheel Adhesion Force for Climbing Robot. Journal of Robotics and Mechatronics, 3, 534-541. doi.org/10.3844/jmrsp.2019.534.541

Younes, T. M., AlKhedher, M. A., SOLIMAN, A. H., & Al Alawin, A. (2019). Design and Implementation of Myoelectric Controlled Arm. Journal of Mechatronics and Robotics, 3(1), 552-562. doi.org/10.3844/jmrsp.2019.552.562